Blockchain-Based Water-Energy Transactive Management with Spatial-Temporal Uncertainties

Pengfei Zhao, *Member, IEEE,* Shuangqi Li*, Graduate Student Member, IEEE*, Paul Jen-Hwa Hu, Chenghong Gu, *Member, IEEE,* Shuai Lu, *Member, IEEE,* Shixing Ding, *Graduate Student Member, IEEE* Zhidong Cao, Da Xie, *Senior Member, IEEE,* and Yue Xiang, *Senior Member, IEEE*

***Abstract*— Water resources are vital to the energy conversion process but few efforts have been devoted to the joint optimization problem which is fundamentally critical to the water-energy nexus for small-scale or remote energy systems (e.g., energy hubs). Traditional water and energy trading mechanisms depend on centralized authorities and cannot preserve security and privacy effectively. Also, their transaction process cannot be verified and is subject to easy tampering and frequent exposures to cyberattacks, forgery, and network failures. Toward that end, water-energy hubs (WEHs) offers a promising way to analyse water-energy nexus for greater resource utilization efficiency.**

We propose a two-stage blockchain-based transactive management method for multiple, interconnected WEHs. Our method considers peer-to-peer (P2P) trading and demand response, and leverages blockchain to create a secure trading environment. It features auditing and resource transaction record management via system aggregators enabled by a consortium blockchain, and entails spatial-temporal distributionally robust optimization (DRO) for renewable generation and load uncertainties. A spatial-temporal ambiguity set is incorporated in DRO to characterize the spatial-temporal dependencies of the uncertainties in distributed renewable generation and load demand. We conduct a simulation-based evaluation that includes robust optimization and the moment-based DRO as benchmarks. The results reveal that our method is consistently more effective than both benchmarks. Key findings include i) our method reduces conservativeness with lower WEH trading and operation costs, and achieves important performance improvements by up to 6.1%; and ii) our method is efficient and requires 18.7% less computational time than the moment-based DRO. Overall, this study contributes to the extant literature by proposing a novel two-stage blockchain-based WEH transaction method, developing a realistic spatial-temporal ambiguity set to effectively hedge against the uncertainties for distributed renewable generation and load demand, and producing empirical evidence suggesting its greater effectiveness and values than several prevalent methods.

***Index Terms*—Blockchain, spatial-temporal ambiguity set, two-stage framework, water-energy nexus.**

This work was supported in part by the New Generation Artificial Intelligence Development Plan of China (2015–2030) (Grants No. 2021ZD0111205), the National Natural Science Foundation of China (Grants No. 72025404, No.71621002, and No. 71974187), Beijing Natural Science Foundation (L192012) and Beijing Nova Program (Z201100006820085). (*Pengfei Zhao and Shuangqi Li are first co-authors and contributed equally to this work.*)

P. Zhao and Z. Cao (corresponding author) are with the State Key Laboratory of Management and Control for Complex Systems, Institute of Automation, Chinese Academy of Sciences, Beijing, China, and School of Artificial Intelligence, University of Chinese Academy of Sciences, Beijing, 100190, China. (email: Pengfei.zhao@ia.ac.cn, Zhidong.Cao@ia.ac.cn).

Shuangqi Li is with the Department of Electrical Engineering, The Hong Kong Polytechnic University, Hong Kong, and the Department of Electronic and Electrical Engineering, University of Bath, Bath, BA2 7AY, U.K. (e-mail: shuangqi.li@connect.polyu.hk)

P. Hu is with the David Eccles School of Business, the University of Utah, Utah, USA. (e-mail: paul.hu@eccles.utah.edu).

C.Gu is with the Department of Electronic & Electrical Engineering, University of Bath, Bath, BA2 7AY, UK.(email: C.Gu@bath.ac.uk).

Shuai Lu is with the School of Electrical Engineering, Southeast University, Nanjing 210096, China (e-mail: lushuai1004@outlook.com)

Shixing Ding is with the School of Cyber Science Engineering, Southeast University, Nanjing 211189, China (e-mail: dingshx616@163.com).

D. Xie is with the Department of Electrical Engineering, Shanghai Jiao Tong University, Shanghai 200240, China (e-mail: xieda@sjtu.edu.cn).

Y. Xiang is with College of Electrical Engineering, Sichuan University, China. (email: xiang@scu.edu.cn).

NOMENCLATURE

A. Sets

T	Time slots.
H	Water energy hubs (WEHs).

B. Parameters

λ^{P}_{h2g}	Unit cost of selling power to the market.
$\lambda^{P/G/W}_{g2h}$	Unit cost of buying market power, gas, water.
$\lambda^{P}_{re}, \lambda^{G}_{re}, \lambda^{W}_{re}$	Reward unit cost of resource trading estimation.
$\lambda^{P}_{h2h}, \lambda^{H}_{h2h}, \lambda^{W}_{h2h}$	Unit cost of resource trading among P2P WEHs.
$\lambda^{BS}_{h}, \lambda^{HS}_{h}, \lambda^{WS}_{h}$	Depreciation unit cost of storage devices.
$\vartheta^{P}_{h2g}, \vartheta^{P}_{g2h}$	Penalty unit cost of power trading difference among two stages.
$\vartheta^{G}_{g2h}, \vartheta^{W}_{g2h}$	Penalty unit cost of gas and water trading difference among two stages.
$\vartheta^{P}_{h2h}, \vartheta^{H}_{h2h}, \vartheta^{W}_{h2h}$	Penalty unit cost of resource trading difference among two stages for WEHs.
$\omega^{\{\cdot\}}_{PoW}$	Cost coefficient of consensus process.
η_e, η_{th}	CHP's power and heating conversion efficiency.
η_f	Efficiency of gas furnace conversion.
η_{COP}	Coefficient of performance.
η^{g}_{p2g}	Conversion efficiency for P2G electrolyser.
η^{h}_{EB}	Conversion efficiency of boiler.
$\eta^{w}_{p2g}, \eta^{w}_{cp}$	Water consumption coefficient.
$G^{i}_{cp,max}$, $P^{i}_{COP,max}$ $G^{i}_{GF,max}, P^{i}_{p2g,max}$	Maximum (max) input of all the energy converters.
$G^{i}_{cp,min}$, $P^{i}_{COP,min}$ $G^{i}_{GF,min}, P^{i}_{p2g,max}$	Minimum (min) input of all the energy converters.
$P^{i}_{EB,max}, P^{i}_{EB,min}$	Max & min input of electric boiler.
$\Theta^{s,ch}_{HS,max/min}$	Max & min charging power of heat storage.
$\Theta^{s,dch}_{HS,max/min}$	Max & min discharging power of heat storage.
$P^{s,ch}_{BS,max/min}$	Max & min charging power.
$P^{s,dch}_{BS,max/min}$	Max & min discharging power.
$E_{BS,max/min}$	Max & min remaining energy of battery.
$\sigma^{s,ch}_{WS,max/min}$	Max & min charging water.
$\sigma^{s,dch}_{WS,max/min}$	Max & min discharging water.
$V_{WS,max/min}$	Max & min remaining water.
$\eta^{ch}_{BS}, \eta^{dch}_{BS}$	Charging and discharging efficiency of battery.
$P^{h2g}_{max/min}$	Max & min buying power from the market.
$P^{g2h}_{max/min}$	Max & min selling power to the market.
$G^{g2h}_{max/min}$	Max & min buying gas from the market.
$\sigma^{g2h}_{max/min}$	Max & min buying water from the market.

$P^{h2h}_{p,max/min}$	Max & min buying power between WEHs.
$P^{h2h}_{s,max/min}$	Max & min selling power of WEHs.
$\Theta^{h2h}_{p,max/min}$	Max & min buying heat between WEHs.
$\Theta^{h2h}_{s,max/min}$	Max & min selling heat between WEHs.
$\sigma^{h2h}_{p,max/min}$	Max & min buying water between WEHs.
$\sigma^{h2h}_{s,max/min}$	Max & min selling water between WEHs.
$\tau_h^{P,max}, \tau_h^{H,max}, \tau_h^{W,max}$	Max load with demand response.
$DR_{P,max}, DR_{H,max}, DR_{W,max}$	Demand response level (%).
$\gamma_{h,t}$	Output forecast of PV generation.
$L^P_{h,t}, L^H_{h,t}, L^W_{h,t}$	Load demand of power, heat and water.

C. Variables

$P^{s,h2g}_{h,t}, P^{s,g2h}_{h,t}$	Selling and buying power with the market.
$G^{s,g2h}_{h,t}, \sigma^{s,g2h}_{h,t}$	Buying gas/water from the market.
$P^{s,h2h}_{h,t,p/s}$	P2P power trading amount of WEHs.
$\Theta^{s,h2h}_{h,t,p/s}$	P2P heat trading amount of WEHs.
$\sigma^{s,h2h}_{h,t,p/s}$	P2P water trading amount of WEHs.
$P^{s,o}_{h,cp,t}, \Theta^{s,o}_{h,cp,t}$	Energy output of CHP.
$P^{s,o}_{h,GF,t}, \Theta^{s,o}_{h,COP,t}, G^{s,o}_{h,p2g,t}, \Theta^{s,o}_{h,EB,t}$	Energy output of gas furnace, GSHP, P2G and boiler.
$\sigma^{s,i}_{h,p2g/cp,t}$	Hydraulic demand of P2G and CHP.
$P^{s,ch}_{h,BS,t}, P^{s,dch}_{h,BS,t}$	(dis)Charging amount of battery devices.
$\Theta^{s,ch}_{h,HS,t}, \Theta^{s,dch}_{h,HS,t}$	(dis)Charging amount of heat storage devices.
$\sigma^{s,ch}_{h,WS,t}, \sigma^{s,dch}_{h,WS,t}$	(dis)Charging of water storage devices.
$E^s_{h,BS,t}, E^s_{h,HS,t}, V^s_{h,WS,t}$	Residual capacity of energy storage devices.
$\varphi^{DR,P}_{h,t}, \varphi^{DR,H}_{h,t}, \varphi^{DR,W}_{h,t}$	Load deviation owing to demand response.
$\tau^P_{h,t}, \tau^H_{h,t}, \tau^W_{h,t}$	Load after demand response.
$\xi_{h,t}$	PV generation uncertainty.
$\zeta_{h,ele}, \zeta_{h,th}, \zeta_{h,w}$	Load uncertainty.

I. INTRODUCTION

A. Research Motivation

ENERGY and water are closely interdependent and can create significant restrictions on each other. Water resources are critical to energy transmission, distribution and conversion [1]. To illustrate, the converted heat in combined heat and power (CHP) often appears in hot water. Power-to-gas (P2G) facilities consume a giant portion of water and split it into hydrogen via electrolyzers [2]. Hydrogen can be fed and stored into natural gas pipes or storage devices, and absorbing carbon dioxide emissions. Furthermore, water facilities consume 3% of the total electric power in the U.S [3]. Toward that end, about 80% of the electric power consumed by water distribution systems is used to pump and distribute water in urban areas. In the existing research, energy and water are mostly modelled and managed separately, which substantially affects the resource usage efficiency.

The emerging multi-energy perspective allows effective ways to enhance energy utilization efficiency [4]. Central to multi-energy carriers are energy hubs that serve as an interface between energy suppliers and consumers [5]. These hubs provide greater operational flexibility through energy conversions. Previous research has shown a desirable efficacy in the trading and operations facilitated by interconnected multi-energy hubs [6, 7]. The dense linkage between water and energy resources underscore the criticality of increasing the overall operational efficiency, especially in light of their increasing synergistic relationship in urban areas. However, water-energy hubs (WEHs) have received little attention and warrant efforts to examine the multiplicity of feedback and interdependency, which jointly influence the sustainability of water-energy nexus in the form of WEHs.

As energy trading is transforming from the centralized management toward a consumer-interactive paradigm, the P2P trading environment for WEHs should be analysed to increase the overall efficiency of the water-energys nexus. Yet, the growing use of data sharing in P2P trading, enabled by advanced information and communication technologies (ICTs), has led to serious security and privacy problems [8, 9]. Instead of a centralized third party that acts as a transaction intermediary, a blockchain can be employed to provide a transparent, secure trading platform; e.g., financial applications [10]. The blockchain distributes data ledgers among autonomous nodes (i.e., entities) and enable smart contracts, with increased trading security [11]. With a blockchain, energy trading data is stored and transmitted as sealed blocks that are linked as a chain. All the entities can verify the chain order to detect data tampering [12]. The use of a blockchain ensures confidentiality and transparency in P2P trading that includes transactions involving multiple energy resources. The consensus mechanism is central to a blockchain, because it audits and records the (trading) information of distinct nodes [13]. This mechanism depicts the dynamically active status of a blockchain and is critical to the resulting reliable and efficient environment that guarantees genuine and safe transactions [14].

The uncertainties in water-energy trading stem from renewable generation, load, and trading prices. They are stochastic in nature, complicate the optimization problem, and likely lead to sub-optimal solutions. This uncertainty-aware decision-making problem is typically modelled as robust optimization (RO) [15, 16] or stochastic optimization (SO) [17, 18]. In general, RO requires little uncertainty information about the predefined uncertainty set and usually leads to excessive robustness [19]. On the other hand, SO either highly depends on historical data or assumes a particular distribution of the uncertainty, and its computational efficiency is an important limitation.

Distributionally robust optimization (DRO) can address the limitations of RO and SO, and has been considered for energy management [20]. It offers a mitigated robust solution within the *ambiguity set* [21] by using it to characterize all possible distributions instead of assuming the availability of an uncertainty distribution [22, 23]. The choice of an optimal ambiguity set should adhere to two principles: the ambiguity set must contain the real distribution and the size of the ambiguity set needs to be minimized. When both principles are satisfied, the optimization problem can be robustified against the real

uncertainty distribution and the computational conservativeness is reduced. Building on these principles, we develop a DRO model that contains structural information about the underlying uncertainty distribution. A new spatial-temporal-based ambiguity set is used to represent the copula constraint and thus further determine the original discrepancy-based ambiguity set. The copula constraint essentially models multivariate dependences, such that the resulting spatial-temporal dependencies can remove the unrealistic uncertainty distributions of renewable generation.

B. Background and Related Works

Optimization modelling of the water-energy nexus is closely relevant to our study. We then review several representative studies of blockchain-based P2P energy trading schemes, and finally summarize the state-of-the-art research on DRO. Previous literature focuses on joint optimization of water-power systems to reduce operation costs and carbon abatement [24-27]. For example, Oikonomou and Parvania [24] study an integrated power-water system (IPWS) and develop an optimal power-water flow management model to excavate operational benefits and flexibilities in water treatment and desalination plants. Li et al. [25] design an optimal demand-side management for IPWSs at the distribution level by using a quasi-convex hull-based technique for intractable nonlinear programming. Mehrjerdi [26] develops a joint optimization of IPWS for remote islands and examines a desalination procedure that includes multi-stage flash and reverse osmosis, and uses a battery system to store excessive renewable generation.

Previous studies also analyse the water-energy scarcity problem in energy shortage and drought scenarios. To test system robustness and resilience in extreme weather, Martinez-Cesena et al. [28] develop a IPWS simulation method to mitigate climate-driven stresses and shocks. This method incorporates a mixed integer linear programming model to examine assumptions that are commonly made by models and methods to simulate the influences of high temperatures on generation capacity. Case studies are conducted in a Ghanaian IPWS. Zuloaga and Vittal [29] design long-term simulations for an IPWS to mitigate the gap between requested water and dispatched supply for hedging against extreme drought conditions. These studies have shed light on optimization of an IPWS but they fall short in coordinating the increasingly complex, coupled, and constrained multi-vector energy systems.

Research on WEH is still an infant field so far, which mostly focuses on optimal operation designs to reduce the operation cost. Pakdel et al. [30] suggest a multi-objective optimization for WEHs to minimize energy costs and the amount of freshwater extracted, using the interdependency between the energy hub and water desalination systems to reduce the renewable spillage. Roustaei et al. [31] design a scenario-based WEH operation scheme for smart islands, which considers the impacts of the microgrid integration and uncertainty factors. To safely feed power, thermal, and water for remote regions, a resilience-based WEH scheduling model is proposed by [32], with the consideration of maintenance impacts. This model introduces the beneficial degree of freedom to guarantee the safe mode of component maintenance programming.

The emerging blockchain technology offers a promising solution to secure trading mechanisms in WEHs. Most previous focuses on blockchain-based P2P energy trading and management for decentralized energy systems. For example, Huang et al. [33] describe a bi-layer energy trading scenario enabled by a multi-blockchain with delegated proof of reputation for microgrids to ensure users can execute their promised transactions completely. Yan et al. [34] apply blockchain to trade energy and carbon allowance for microgrids, using a scalable payoff allocation method for co-operative game formulation. Huang et al. [35] suggest scalable blockchain-based energy trading for cooperative microgrids, consisted of data, consensus, and application layers. A redundant data exchange strategy is used to scale block creation. Yang and Wang [36] create a blockchain-based energy trading model to attain socially optimal solutions with ensured safety, and test the model with a prototype blockchain system implemented on a hardware platform. Hua et al. [37] design a blockchain-based P2P scheme that integrates negotiation-oriented auctions and pricing mechanisms in local energy markets. A Stackelberg cooperative game model is developed to aggregate energy retailers and prosumers. To incentivize prosumers for energy savings, Abdelsalam et al. [38] take a percentage power change approach to allow a blockchain to preserve trading information until no sensitive information is shared. Xu et al. [39] propose a trustworthy dispatch model for distribution energy systems, which considers a high penetration of electric vehicles and renewable generation. An orderly charging iteration optimization algorithm is applied to records and verifications in the blockchain.

Furthermore, DRO considers the occurrences of various uncertainty scenarios as imprecise data that follow an ambiguous distribution rather than a deterministic distribution [40]. Moment-[41, 42] and discrepancy-based [43, 44] constitute two major types of DRO. Most early DRO models apply a moment-based ambiguity set that provides limited moment information and support. For example, Lu et al. [45] design an electric vehicle management model for distribution firms. The model employs moment-based DRO to capture the impacts of vehicle mobility and seeks to minimize them. Mean vectors and covariance matrices are included as additional moment information and a tractable semidefinite programming model is then reformulated. Ding et al. [46] use the mean, symmetric, and unimodal of different ambiguity sets to characterize the stochastic nature of renewable generation and contingencies. Yang et al. [47] provide a less conservative solution by developing a frequency constrained multi-energy system optimization in combination with wind uncertainty, which considers the joint chance constraints in second-order moment and unimodality.

Discrepancy-based models define the ambiguity sets as a ball within a certain measured space of uncertainty distributions [48, 49]. Toward that end, Li et al. [50] target microgrid operations and exploit the Wasserstein metric to construct the ambiguity set for uncertain renewable generation and load consumption. They use the Wasserstein radius to quantify the vicinity of support points. Che et al. [51] suggest a strategic operation for heating, ventilation, and air-conditioning systems, which enhances operational efficiency by incorporating a discrepancy-based ambiguity set, in the presence of unavoidable forecasting errors of temperature. To enhance the computational efficiency (i.e., speed), a separation method is applied to perform off-line computations of the counterparts in chance constraints. Chu et al. [52] suggest a microgrid scheduling approach that considers system frequency

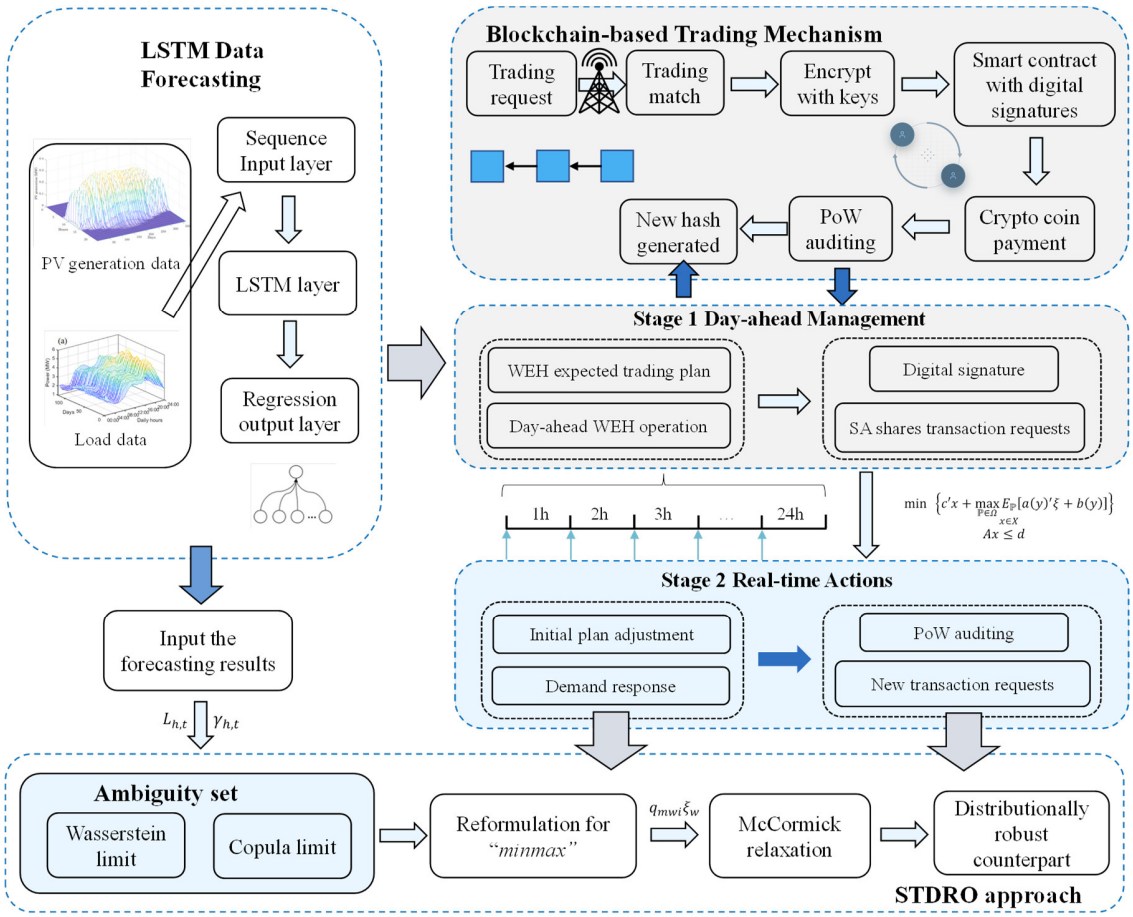

Fig. 1. Schematic overview of the reported study.

dynamics, which employs an ambiguity set to model the noncritical load with second-order moment information. In [53], a hybrid Wasserstein metric-moment ambiguity set is constructed to capture uncertain contingencies for integrated power and heat systems. The recast problem under l_∞ norm is then efficiently solved by a modified column-and-constraint generation algorithm.

A review of related literature indicates several important gaps that we seek to address. First, despite the increasing attention to water-energy nexus, optimization and transactive management of WEHs that considers complex and intrinsic interdependencies in the hub level are lacking. Effective P2P water-energy trading mechanisms are especially pivotal to efficient coordination of multiple, interconnected WEHs. Second, data security is crucial, due to the fast-growing cyber-attacks. In that regard, blockchain-based urban WEH transactive management is promising, avoids exclusive reliance on a trusted third party, but remains understudied. Third, traditional DRO uses a minimal set of historical data to model uncertainties, which is prone to yielding excessively conservative solutions. This reveals the need for methods capable of enhancing solution optimality and enriching the modeling of ambiguity sets.

C. *Key Contributions*

We propose an innovative blockchain-based transactive co-optimization of WEHs, which considers P2P trading and demand response, using a consortium blockchain for privacy-preserving trading and operation mechanism. Each WEH represents as an automatous entity that consumes and trades water and energy with other WEHs or the system aggregator (SA). To be qualified for trading of water, power, heating, and gas, a WEH needs to be registered with a unique key and certificate using crypto coins. Transaction record auditing and sharing to the public are managed by SAs rather than being intermediated by a centralized third party. The proposed two-stage operation method allows trading with external water and energy markets in the day-ahead stage. The second (real-time) stage features blockchain-based P2P trading among interconnected WEHs. Multi-vector demand response are considered in this stage, so WEHs can actively participate in response to fluctuating prices in external markets. Our spatial-temporal DRO considers uncertain weather conditions, user-side load fluctuations, variations in renewable generation and load demand. These uncertainties are captured by an ambiguity set constructed with copula information. Compared with existing discrepancy-based ambiguity sets, this copula-based spatial-temporal ambiguity set effectively incorporates spatial-temporal dependencies and avoids unrealistic uncertainty distributions.

The proposed blockchain-based WEH management is novel and valuable. Our study makes several important contributions:

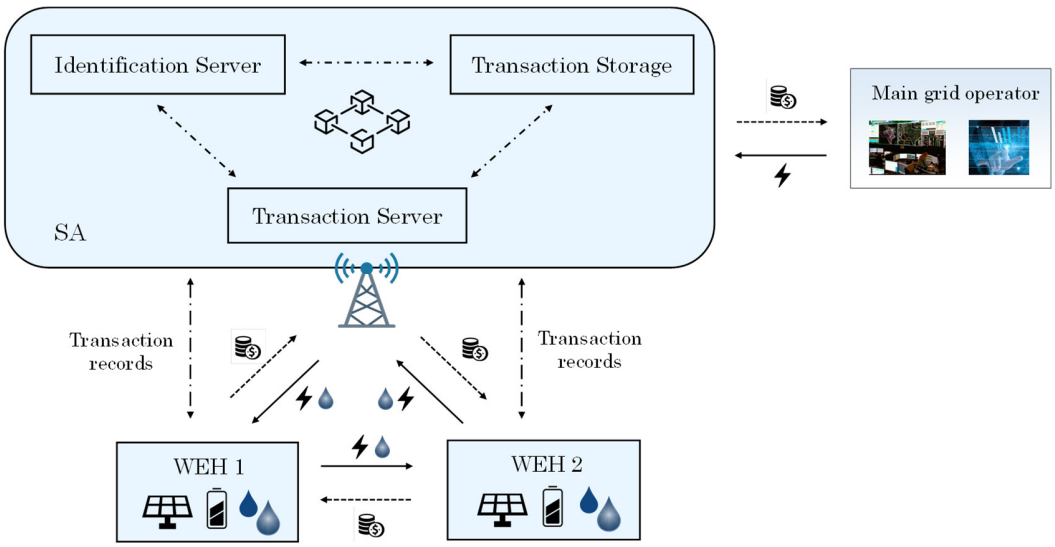

Fig. 2. Proposed trading mechanism.

1. Water-energy nexus management: We develop a novel two-stage water-energy nexus management that involves WEHs, which adds to previous research in two essential aspects: i) the water-energy nexus we formulate is appropriate and crucial for WEHs in small-scale communities (e.g., residential areas), while many prior studies target meta-analyses or resource allocation problems for water-energy nexus at the country or grid level [54-56]; ii) the intricate water-energy nexus among water, power, gas, and heat aims to achieve system optimality by allocating interactives in resource usages [28, 57] and helps ensure transparent, safe P2P transactions among WEHs. The transactive management also increases operational flexibility and resource utilization efficiency.

2. Blockchain-based trading mechanism: We create a consortium blockchain for secure water-energy trading and information sharing. The necessary consensus is incorporated in the proposed method's second stage to audit transactions that then are used to link and update blocks in the existing chain. The blockchain-based trading mechanism is advantageous since it is embedded in the proposed two-stage optimization framework. The WEH owners are able to submit initial day-ahead transaction requests and adjust their decisions the next day.

3. Spatial-temporal ambiguity set: To capture variations in renewable generation, our DRO includes a spatial-temporal ambiguity set, which is constructed with copula information, to separate the joint distribution and create marginal distributions and dependence structures. The inclusion of correlation information can enhance discrepancy-based DRO by removing erroneous distributions.

4. Cross-vector demand response: A cross-vector demand response is incorporated to encourage and foster intelligent consumptions of water and energy loads, which in turn reduces operation costs and contributes to water and energy savings.

D. Paper Organization

The rest of the paper is organized as follows. Section II presents the problem formulation. The solution approach for solving the two-stage spatial-temporal DRO is given in section III. Section IV discusses simulation results and the conclusion is drawn in section V.

II. Problem Formulation

This section presents the blockchain-based transactive management model of WEHs firstly, followed by introducing the system structure of WEH. Then the day-ahead and real-time models are proposed in sections C and D, respectively. In Fig. 1, the schematic overview of the entire paper is given.

A. Blockchain-based Transactive Management

The water-energy trading is manipulated not only between different WEHs, but also between WEHs and SAs. During the first stage, the main grid operator (MGO), who is responsible for the urban water and energy grids, determines the initial operation planning according to the day-ahead trading estimation by WEH owners. WEH owners are motivated and recompensed to share the expected next-day trading specification with SAs, which contributes to the optimal and accurate operation decision made by the MGO. The pre-determined trading scheme should be encrypted and signed with digital signatures for securing the transaction. The MGO receives the pseudonym information from SAs, followed by the reserve schedule of energy units based on the collected water-energy trading plan from SAs. The second stage requires the WEH owners to send another water-energy trading request due to the uncertain renewable generation and load. The MGO then takes corrective actions to mitigate the uncertain trading manner.

The step-by-step blockchain-based trading mechanism is illustrated in Fig. 1. SAs receive the trading requests from WEHs and broadcast them to all the WEH owners and the MGO. There is a consensus procedure in the second stage for transaction audits, which is the responsibility for all the authorized SAs. As shown in Fig. 2, an SA is composed of a transaction storage and server, and an identification server. We use the transaction server to collect trading requests from WEHs. The trading pairs are then matched for all the registered WEHs. The identification server is adopted to manage the account information of WEHs. It also ciphers and forms transactions into blocks followed by the transmission to all the SAs for auditing. The transaction records are saved in the transaction storage section. Each transaction record is encrypted with a unique timestamp and digital signatures are required. WEH owners are able to submit a trading request for either the following 24 hours or conduct the real-time adjustment. We compile smart contras via Solidity 0.8.7 with the code shown in Fig. 3. We provide a flowchart of the smart contract in Fig. 4 [58, 59]. External,

digital data are input to the contract, together with the predetermined trigger conditions. The state machine and the contract transaction set are used to assess and dock the external information.

```
pragma solidity ^0.8.7;

contract FeeCollector { // 0xA182D684c4e930142b97986Eb7fe0Cb40D1D929d
    address public owner;
    uint256 public balance;

    constructor() {
        owner = msg.sender; // store information who deployed contract
    }

    receive() payable external {
        balance += msg.value; // keep track of balance (in WEI)
    }


    function withdraw(uint amount, address payable destAddr) public {
        require(msg.sender == owner, "Only owner can withdraw");
        require(amount <= balance, "Insufficient funds");

        destAddr.transfer(amount); // send funds to given address
        balance -= amount;
    }
}
```

Fig. 3. Deployed smart contract code via Solidity.

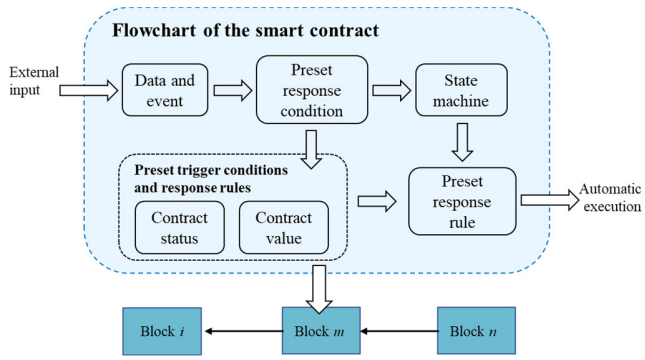

Fig. 4. Flowchart of the proposed smart contract.

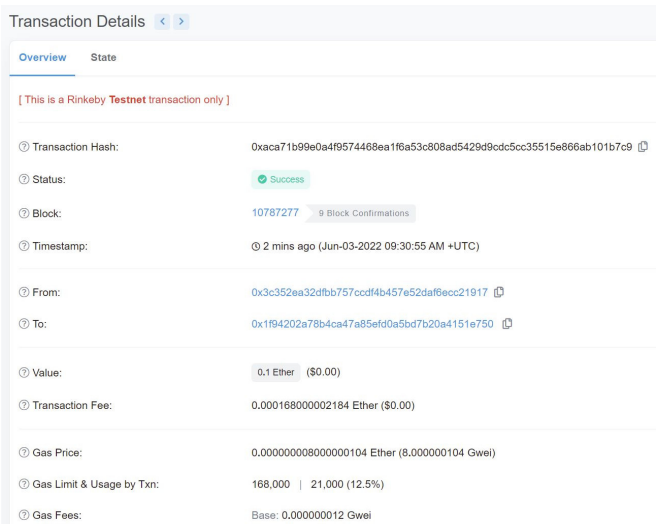

Fig. 5. Submitted water-energy request from WEH1.

Once a transaction is authorized by the SA, the transaction is completed. In Fig. 5, the figure shows the hash codes of transactions and the blocks where the corresponding transactions are included. The addresses of the contract sender and receiver are also recorded. The hash guarantees this trade is publicly traceable and verified by the SA community for viewing and auditing. Each WEH is registered via a trusted authority with a unique identity ID_h, which is thus legitimate for secure and safe trading. The public and private keys (PUK_h and PRK_h), and certificates (C_h) are coupled with ID_h. The crypto coin is used as an online ledger with cryptography to secure transactions. Each ID_h has a digital wallet with the wallet address W_h and a mappling lits $\{PUK_h, PRK_h, C_h, W_h\}$ which is provided by the registration authority. The WEH owner can decide to trade with other WEHs, the MGO or not participate in the trading. Pseudonyms are generated for participators for every transaction.

When trading is agreed, the buying side makes the payment via crypto coins. The buying side drafts the transaction record, waiting for the verification and signature from the selling side. When a trade is agreed, the buying side makes a payment using crypto coins. In addition, the buying side drafts the transaction record, and waits for verification and signature from the selling side. This trade then is uploaded to all the authorized SAs for auditing, which provides a proof-of-X (PoX) mechanism, where X can refer to anything. Essentially, PoX ensures all decentralized participants' ability to secure the transaction. Exemplary PoX mechanisms include proof-of-work, proof-of-stake, proof-of-burn, and proof-of-inclusion [60, 61].

A unique hash of each block is created by the PoW. The cryptographic hash provides the main secure guarantee for the blockchain as the linkage between each block. To tamper the block's content, the hash with difficulty needs to be disconnected first. After a transaction is successfully added to the consortium blockchain, it is structured into a block and linked with the existing blockchain. The record is publicly visible to all the WEHs and SAs.

B. System Structure of WEH

The WEH structure is shown in Fig. 6, which is composed of water-energy supply, converters, storage systems, a PV generator, and consumption. Each WEH can be supplied from the external markets or other interconnected WEHs. CHP generates heat and power simultaneously with gas supply. P2G converts power to hydrogen gas, which is of high efficiency and enables to reduce carbon emission. The ground source heat pump (GSHP) transfers to heat from power with the ground as the media. Gas furnaces and electric boilers utilize gas and power to produce heat. The proposed WEH considers a hybrid storage system to store power, heat, and water, which is extensively utilized to facilitate P2P trading and demand response. Apart from the local water-energy consumption, excessive resources can be traded within the P2P trading environment.

C. Day-Ahead Transactive Management

The day-ahead transactive co-optimization is to be minimized in the first stage. The day-ahead objective is given in (1). The first term of (1) shows the reward for selling power to the MGO. Trade with external markets is determined in the day-ahead stage. Therefore, the second to fourth terms are the estimated purchase of water and energy. Next day estimation of load consumption and trading are encouraged by the MGO because it is beneficial for reducing the difficulties of the main grid management. The day-ahead trading estimation reward is given in the fifth and sixth terms. The lack of day-ahead water and energy purchase due to the

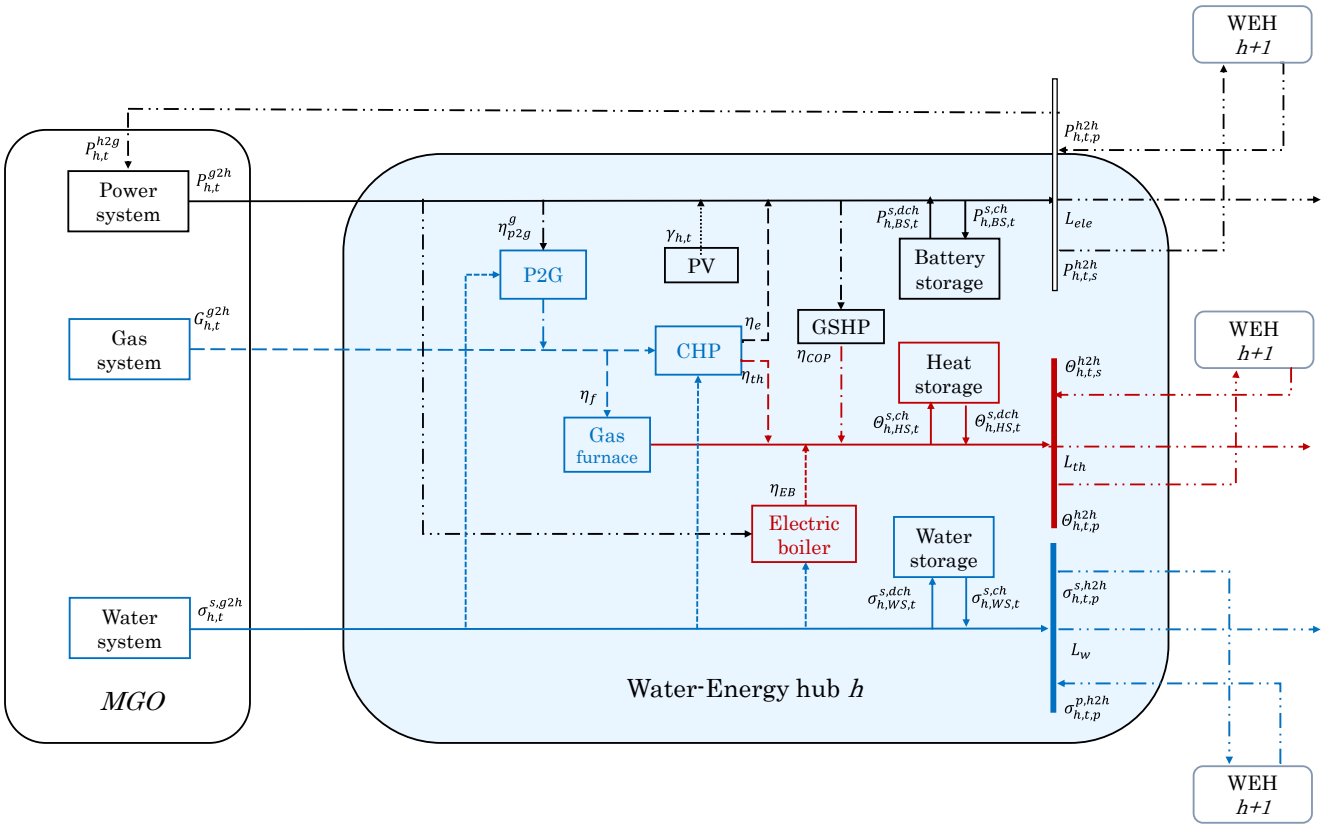

Fig. 6. Structure of the proposed WEH.

wrongly estimated usage may lead to insufficient supply, which can be resolved by P2P trading or purchase from the real-time external market with a higher price. The final three terms are the degradation costs of the hybrid storage system.

$$\begin{aligned}\Gamma_1 = \min \sum_{h\in H,t\in T} & -\lambda^P_{h2g} P^{s,h2g}_{h,t} \\ & + \lambda^P_{g2h} P^{s,g2h}_{h,t} + \lambda^G_{g2h} G^{s,g2h}_{h,t} + \lambda^W_{g2h} \sigma^{s,g2h}_{h,t} \\ & - \lambda^P_{re}\left(P^{s,h2g}_{h,t} + P^{s,g2h}_{h,t}\right) - \lambda^G_{re} G^{s,g2h}_{h,t} \\ & + \lambda^{BS}_h\left(P^{s,ch}_{h,BS,t} + P^{s,dch}_{h,BS,t}\right) + \lambda^{HS}_h\left(P^{s,ch}_{h,HS,t} + P^{s,dch}_{h,HS,t}\right) \\ & + \lambda^{WS}_h\left(\sigma^{s,ch}_{h,WS,t} + \sigma^{s,dch}_{h,WS,t}\right)\end{aligned} \tag{1}$$

1) Conversion Constraints

The converter operational constraints are shown in (2)-(11). Constraint (2) presents the heat output of GSHP. Equation (3) shows the output expression of P2G. Constraint (4) models the water consumption of P2G. The constraints of the gas furnace, electric boiler are given in (5)-(7). For CHP, the power and heat output are shown in (8) and (9), respectively, followed by the water consumption constraint in (10). Constraint (11) limits the input of all the energy converters.

$$\Theta^{s,o}_{h,COP,t} = \eta_{COP} P^{s,i}_{h,COP,t} \tag{2}$$

$$G^{s,o}_{h,p2g,t} = \eta^g_{p2g} \frac{P^{s,i}_{h,p2g,t}}{\Omega_{hy}} \tag{3}$$

$$\sigma^{s,i}_{h,p2g,t} = \eta^w_{p2g} P^{s,i}_{h,p2g,t} \tag{4}$$

$$P^{s,o}_{h,GF,t} = \eta_{GF} G^{s,i}_{h,GF,t} \tag{5}$$

$$\Theta^{s,o}_{h,EB,t} = \eta^h_{EB} P^{s,i}_{h,EB,t} \tag{6}$$

$$\sigma^{s,i}_{h,EB,t} = \eta^w_{EB} P^{s,i}_{h,EB,t} \tag{7}$$

$$P^{s,o}_{h,cp,t} = \eta^e_{cp} G^{s,i}_{h,cp,t} \tag{8}$$

$$\Theta^{s,o}_{h,cp,t} = \eta^h_{cp} G^{s,i}_{h,cp,t} \tag{9}$$

$$\sigma^{s,i}_{h,cp,t} = \eta^w_{cp} G^{s,i}_{h,cp,t} \tag{10}$$

$$P^i_{\{\cdot\},min} \le P^{s,i}_{h,\{\cdot\},t} \le P^i_{\{\cdot\},max}, \{\cdot\} = COP, p2g, GF, EB, cp \tag{11}$$

2) Storage Constraints

The constraints of the hybrid storage system are shown in (12)-(20), including the i) limits of charging and discharging power, heat and water, ii) remaining storage capacity expression and iii) maximum limits of remaining storage capacity.

$$P^{s,ch/dch}_{BS,min} \le P^{s,ch/dch}_{h,BS,t} \le P^{s,ch/dch}_{h,BS,max} \tag{12}$$

$$E^s_{h,BS,t} = E^s_{h,BS,t-1} + \sum_1^t P^{s,ch}_{h,BS,t}\eta^{ch}_{BS} - P^{s,dch}_{h,BS,t}/\eta^{dch}_{BS} \tag{13}$$

$$E_{BS,min} \le E^s_{h,BS,t} \le E_{BS,max} \tag{14}$$

$$\Theta^{s,ch/dch}_{HS,min} \le \Theta^{s,ch/dch}_{h,HS,t} \le \Theta^{s,ch/dch}_{h,HS,max} \tag{15}$$

$$E^s_{h,HS,t} = E^s_{h,HS,t-1} + \sum_1^t \Theta^{s,ch}_{h,HS,t}\eta^{ch}_{HS} - \Theta^{s,dch}_{h,HS,t}/\eta^{dch}_{HS} \tag{16}$$

$$E_{HS,min} \le E^s_{h,HS,t} \le E_{HS,max} \tag{17}$$

$$\sigma^{s,ch/dch}_{WS,min} \le \sigma^{s,ch/dch}_{h,WS,t} \le \sigma^{s,ch/dch}_{WS,max} \tag{18}$$

$$V^s_{h,WS,t} = V^s_{h,WS,t-1} + \sum_1^t \sigma^{s,ch}_{h,WS,t} - \sigma^{s,dch}_{h,WS,t} \tag{19}$$

$$V_{WS,min} \le V^s_{h,WS,t} \le V_{WS,max} \tag{20}$$

3) Trading with The External Market

In the day-ahead transactive management, WEH operators can trade with the external market for preparing the next-day supply. Above all, values of $P^{s,h2g}_{h,t}$, $P^{s,g2h}_{h,t}$, $G^{s,g2h}_{h,t}$, and $\sigma^{s,g2h}_{h,t}$

need to be limited. In (21)-(23), balancing conditions for power, gas, heat, and water are presented, respectively.

$$P_{h,t}^{s,g2h} + P_{h,cp,t}^{s,o} + P_{h,BS,t}^{s,dch} + \gamma_{h,t} = P_{h,COP,t}^{s,o} + P_{h,BS,t}^{s,ch} + P_{h,t}^{s,h2g} + P_{h,p2g,t}^{s,i} + P_{h,EB,t}^{s,i} + L_{h,t}^{P} \quad (21)$$

$$G_{h,t}^{s,g2h} + G_{h,p2g,t}^{s,o} = G_{h,GF,t}^{s,i} + G_{h,cp,t}^{s,i} \quad (22)$$

$$\Theta_{h,cp,t}^{s,o} + \Theta_{h,COP,t}^{s,o} + \Theta_{h,HS,t}^{s,dch} + \Theta_{h,EB,t}^{s,o} = \Theta_{h,HS,t}^{s,ch} + L_{h,t}^{H} \quad (23)$$

$$\sigma_{h,t}^{s,g2h} + \sigma_{h,WS,t}^{s,dch} = \sigma_{h,WS,t}^{s,ch} + L_{h,t}^{W} + \sigma_{h,p2g,t}^{s,i} + \sigma_{h,cp,t}^{s,i} + \sigma_{h,EB,t}^{s,i} \quad (24)$$

D. Real-time Transactive Management

The objective function of real-time model is given in (25), containing i) the P2P trading cost among interconnected WEHs, ii) the penalty cost of trading with the external markets, and iii) the consensus cost for PoW mechanism. The penalty cost is used to limit the real-time purchase from the markets. When the day-ahead purchase is insufficient, the penalty cost is regarded as the purchase from the real-time external market with a higher price. On the contrary, the over-purchase from the day-ahead market is also regulated as P2P purchase is considered as the priority when the external supply is insufficient.

$$\begin{aligned} \Gamma_2 = \min \sum_{h\in H, t\in T} & \lambda_{h2h}^{P}\left(P_{h,t,p}^{s,h2h} - P_{h,t,s}^{s,h2h}\right) + \lambda_{h2h}^{H}\left(\Theta_{h,t,p}^{s,h2h} - \Theta_{h,t,s}^{s,h2h}\right) \\ & + \lambda_{h2h}^{W}\left(\sigma_{h,t,p}^{s,h2h} - \sigma_{h,t,s}^{s,h2h}\right) + \vartheta_{h2g}^{P}\left|P_{h,t}^{s,h2g} - P_{h,t}^{r,h2g}\right| + \vartheta_{g2h}^{P}\left|P_{h,t}^{s,g2h} - P_{h,t}^{r,g2h}\right| \\ & + \omega_{PoW}^{P}\left(P_{h,t}^{r,h2g} + P_{h,t}^{r,g2h} + P_{h,t,p}^{r,h2h} + P_{h,t,s}^{r,h2h}\right) + \omega_{PoW}^{H}\left(\Theta_{h,t,p}^{r,h2h} + \Theta_{h,t,s}^{r,h2h}\right) \\ & + \omega_{PoW}^{G} G_{h,t}^{r,g2h} + \omega_{PoW}^{W}\left(\sigma_{h,t}^{r,g2h} + \sigma_{h,t,p}^{r,h2h} + \sigma_{h,t,s}^{r,h2h}\right) \end{aligned} \quad (25)$$

1) P2P Trading and Cross-Vector Demand Response

In real-time transactive management, P2P trading among power, heat, and water is scheduled. Above all, we need to ensure the trading amount ($P_{h,t,p/s}^{s,h2h}$, $\Theta_{h,t,p/s}^{s,h2h}$, $\sigma_{h,t,p/s}^{s,h2h}$) is within the predefined limits. This paper adopts a cross-vector demand response as a viable option to facilitate the active participation of WEHs in shifting the load profile of power, heat, and water, which is inspired by the integrated demand response in [62, 63]. Demand response can guide WEH users with a rational and reasonable transfer of water and energy resources to stabilize peak and valley load consumption. Accordingly, a lower energy consumption cost can be achieved with a load peak shift. The pricing-based demand response program is applied [64, 65] with a real-time pricing (RTP) tariff scheme. Based on the users' price sensitivity, the original demand is affected by the price fluctuation. However, existing literature ignores the demand response of water to further enhance the flexibility of system operation and thus fail to promote the interaction among water and energy. Therefore, the cross-vector demand response is central to encourage the active consumption changing behaviours of water and energy and facilitate the energy substitution effect.

Equation (26) presents the altered WEH load profile of power, heat, and water with the maximum limit shown in (27). Constraint (28) limits the load deviation of demand response participation. Finally, constraint (29) is used to ensure the total load deviation is zero, which indicates that the load consumption is only shifted without curtailment.

$$\tau_{h,t}^{\{\cdot\}} = \zeta_{h,t}^{\{\cdot\}} + \varphi_{h,t}^{DR,\{\cdot\}}, \{\cdot\} = P, H, W \quad (26)$$

$$\tau_{h,t}^{\{\cdot\}} \le \tau_{h}^{\{\cdot\},max}, \{\cdot\} = P, H, W \quad (27)$$

$$\left|\varphi_{h,t}^{DR,\{\cdot\}}\right| \le \zeta_{h,t}^{\{\cdot\}} DR_{\{\cdot\},max}, \{\cdot\} = P, H, W \quad (28)$$

$$\sum_{t=1}^{T} \varphi_{h,t}^{DR,\{\cdot\}} = 0, \{\cdot\} = P, H, W \quad (29)$$

2) Balancing Conditions

The real-time model takes adjustive recourse actions with respect to the parameter changes. Intuitively, due to the P2P trading, demand response program, and uncertainties considered in the second stage, the new balancing conditions of power, gas, heat, and water are given in (30)-(33). The rest of the second-stage constraints are the same as those of the first-stage constraints in (2)-(24) when the superscript '*s*' is replaced by '*r*', which represent '*scheduled*' and '*regulated*', respectively.

$$P_{h,t}^{r,g2h} + \sum_{h\in H} P_{h,t,p}^{r,h2h} + P_{h,cp,t}^{r,o} + P_{h,BS,t}^{r,dch} + \xi_{h,t} = P_{h,COP,t}^{r,o} + \sum_{h\in H} P_{h,t,s}^{r,h2h} + P_{h,BS,t}^{r,ch} + P_{h,t}^{r,h2g} + \tau_{h,t}^{P} \quad (30)$$

$$G_{h,t}^{r,g2h} = G_{h,GF,t}^{r,i} + G_{h,cp,t}^{r,i} \quad (31)$$

$$\sum_{h\in H} \Theta_{h,t,p}^{r,h2h} + \Theta_{h,cp,t}^{r,o} + \Theta_{h,COP,t}^{r,o} + \Theta_{h,HS,t}^{r,dch} = \sum_{h\in H} \Theta_{h,t,s}^{r,h2h} + \Theta_{h,HS,t}^{r,ch} + \tau_{h,t}^{H} \quad (32)$$

$$\sigma_{h,t}^{r,g2h} + \sum_{h\in H} \sigma_{h,t,p}^{r,h2h} + \sigma_{h,WS,t}^{r,dch} = \sum_{h\in H} \sigma_{h,t,s}^{r,h2h} + \sigma_{h,WS,t}^{r,ch} + \tau_{h,t}^{W} + \sigma_{h,p2g,t}^{r,i} + \sigma_{h,cp,t}^{r,i} + \sigma_{h,EB,t}^{r,i} \quad (33)$$

III. Spatial-Temporal Distributionally Robust Optimization Method

The proposed spatial-temporal ambiguity set is first introduced before reformulating the complex *min-max* problem with dualization actions. The proposed method aims to derive the optimal result from the worst-case distribution under the expected manner. We thus formulate the original objective function in a *min-max* framework:

$$\min_{x\in X} \left\{ c'x + \max_{\mathbb{P}\in\Omega} E_{\mathbb{P}}[a(y)'\xi + b(y)] \right\} \quad (34)$$

$$Ax \le d \quad (35)$$

Where x and y represent the decision variables of the first and second stages, $a(y)$ and $b(y)$ are the coefficient vectors of the objective function (34), $\xi \in \mathbb{R}^{|S|}$ stands for the uncertainty parameter, which belongs to probability distribution $\mathbb{P}\left(\mathbb{R}^{|S|}\right)$.

A. Spatial-Temporal Ambiguity Set

The ambiguity set contains a family of distributions, which characterizes the occurrence of all the possible uncertainty-aware scenarios. A discrepancy-based ambiguity set Ω_D is defined as (36) containing distribution p close to the empirical distribution $\mathbb{P}_{ref}$, where $D_{\xi}\left(\mathbb{P}\middle\|\mathbb{P}_{ref}\right)$ is the distributional distance; η is the radius of the ambiguity set. The empirical distribution $\mathbb{P}_{ref}$ is given as (37), where $\hat{\xi}_i$ represents the historical observations; $\theta_{\hat{\xi}_i}$ represents the Dirac distribution; *i* is the index among the *N* historical samples.

$$\Omega_D = \left\{\mathbb{P} \in D_{\xi} \middle| D_{\xi}\left(\mathbb{P}\middle\|\mathbb{P}_{ref}\right) \le \eta\right\} \quad (36)$$

$$\mathbb{P}_{ref} = \frac{1}{N}\sum_{i=1}^{N} \theta_{\hat{\xi}_i} \quad (37)$$

The discrepancy-based ambiguity set enables to incorporate the neighbourhood of the nominal distribution. However, it may accommodate erroneous distributions, i.e., it cannot limit the shape of the distribution and the dependence structure information cannot be reflected. To this end, it will lead to unnecessary over-conservative decisions. To avoid modelling the erroneous distributions, we further incorporate the copula limit in the ambiguity set (38).

$$\Omega_{ST} = \left\{ \mathbb{P} \in P_0\left(\mathbb{R}^{|S|}\right) \middle| \begin{matrix} D_\xi\left(\mathbb{P} \middle\| \mathbb{P}_{ref}\right) \le \eta \\ D_\xi\left(\mathbb{C} \middle\| \mathbb{C}_{ref}\right) \le \gamma \end{matrix} \right\} \tag{38}$$

The distribution information of any multivariate distributions can be decomposed into a collection of marginal distributions and a copula. The distributional distance between the candidate copula $\mathbb{C}$ and the empirical copula $\mathbb{C}_{ref}$ is constrained within γ to guarantee the fixed dependence structure property.

B. Tractable Mathematical Reformulations

For notation brevity, the inner worst-case expectation of (34) is solely given as (39), where $\Xi(x,\xi) = a(x)'\xi + b(x)$.

$$\max_{\mathbb{P}\in\Omega_{ST}} E_{\mathbb{P}}[\Xi(x,\xi)] \tag{39}$$

Subject to

$$D_\xi\left(\mathbb{P} \middle\| \widehat{\mathbb{P}}_N\right) \le \eta \tag{40}$$

$$D_\xi\left(\mathbb{C} \middle\| \widehat{\mathbb{C}}_N\right) \le \gamma \tag{41}$$

Assuming that distribution $\mathbb{P}$ is discrete with a sufficiently large number of samples, the probability distribution can be defined as (42), where $\mathbb{P}_m$ is the endogenous probability and $\theta_{\hat{\xi}_m}$ is the Dirac distribution. Equation (39) can be reformulated into (42)-(47). The original discrepancy functions are reformulated as (44)-(47), where ϑ_{mi} and δ_{mi} are the transportation coefficients of the optimal transport mapping.

$$\mathbb{P} = \sum_{m=1}^{M} \mathbb{P}_m \theta_{\hat{\xi}_m} \tag{42}$$

$$\max_{\mathbb{P}_m\in\Omega_{ST}} \sum_{m=1}^{M} \Xi(x,\xi_m)\mathbb{P}_m \tag{43}$$

$$\text{subject to } \min \sum_{m=1}^{M}\sum_{i=1}^{N} D_\xi\left(\hat{\xi}_i \| \xi_m\right)\vartheta_{mi} \le \eta \tag{44}$$

$$\sum_{m=1}^{M} \vartheta_{mi} = \left(\widehat{\mathbb{P}}_N\right)_i, \sum_{i=1}^{N} \vartheta_{mi} = \mathbb{P}_m \tag{45}$$

$$\min \sum_{m=1}^{M}\sum_{i=1}^{N} D_{\xi^\Phi}\left(\hat{\xi}_i \| \xi_m\right)\delta_{mi} \le \gamma \tag{46}$$

$$\sum_{m=1}^{M} \delta_{mi} = \left(\widehat{\mathbb{C}}_N\right)_i, \sum_{i=1}^{N} \delta_{mi} = \mathbb{C}_m \tag{47}$$

We then eliminate the '*min*' operator due to the '$\le$' constraint. The reformulation of (43)-(47) is given as:

$$\max_{\vartheta_{mi},\delta_{mi}} \sum_{m=1}^{M}\sum_{i=1}^{N} \Xi(x,\xi_m)\vartheta_{mi} \tag{48}$$

$$\text{subject to} \sum_{m=1}^{M}\sum_{i=1}^{N} D_\xi\left(\hat{\xi}_i \| \xi_m\right)\vartheta_{mi} \le \eta : \zeta \tag{49}$$

$$\sum_{m=1}^{M} \vartheta_{mi} = \frac{1}{N}\sum_{i=1}^{N} I_{\xi\ge\hat{\xi}_{wi}}, I_{\xi\ge\hat{\xi}_{wi}} = \begin{cases} 1\ \xi \ge \hat{\xi}_{wi} \\ 0\ \text{Otherwise} \end{cases}, \forall i \in \{1,\dots,N\} : \theta_i \tag{50}$$

$$\sum_{m=1}^{M}\sum_{i=1}^{N} D_{\xi^\Phi}\left(\hat{\xi}_i \| \xi_m\right)\delta_{mi} \le \gamma : \nu \tag{51}$$

$$\sum_{m=1}^{M} \delta_{mi} = \frac{1}{N}, \forall i \in \{1,\dots,N\} : \tau_i \tag{52}$$

We then dualize (48-52) to obtain the '*min*' objective, where ζ, θ_i, ν, and τ_i are the dual variables.

$$\min_{\zeta,\nu\ge0,\theta_i,\tau_i,\chi_m} \zeta\,\eta + \nu\gamma + \frac{1}{N}\sum_{i=1}^{N}\theta_i + \frac{1}{N}\sum_{i=1}^{N}\tau_i \tag{53}$$

Subject to

$$\theta_i \ge \max_{\xi_m,\chi_m} \Xi(x,\xi_m) - \zeta\, D_\xi\left(\hat{\xi}_i \| \xi_m\right) \tag{54}$$

$$\tau_i \ge \max_{\xi_m,\chi_m} -\nu\, D_{\xi^\Phi}\left(\hat{\xi}_i \| \xi_m\right) \tag{55}$$

The distance functions of (54) and (55), i.e., D_ξ and D_{ξ^Φ}, can be defined by norms in (56) and (57), where $\Phi(\cdot)$ stands for the marginal cumulative distribution function.

$$D_\xi\left(\hat{\xi}_i \| \xi_m\right) = \left\|\hat{\xi}_i - \xi_m\right\| \tag{56}$$

$$D_\xi\left(\hat{\xi}_i \| \xi_m\right) = \left\|\Phi\left(\hat{\xi}_i\right) - \Phi(\xi_m)\right\| \tag{57}$$

We can thus merge equations (54) and (55) into (58) combining (56) and (57).

$$\theta_i + \tau_i \ge \max_{\xi_m,\chi_m} \Xi(x,\xi_m) - \zeta D_\xi \left\|\hat{\xi}_i - \xi_m\right\| - \nu\, D_{\xi^\Phi}\left\|\Phi\left(\hat{\xi}_i\right) - \Phi(\xi_m)\right\| \tag{58}$$

In order to eliminate the norms, equation (58) is derived by the dual norm reformulation:

$$\theta_i + \tau_i \ge \max_{\xi_m,\chi_m} \Xi(x,\xi_m) - \zeta\ \kappa_i' D_\xi\left(\hat{\xi}_i - \xi_m\right) - \nu\, D_{\xi^\Phi}\left\|\Phi\left(\hat{\xi}_i\right) - \Phi(\xi_m)\right\| \tag{59}$$

$$\|\kappa_i\|_* \le \zeta, \|\varsigma_i\|_* \le \nu \tag{60}$$

The function $\Xi(x,\xi_m)$ can be represented by the indicator function (61), where w stands for the total number of the uncertainty sources, i.e., w renewable power generators in this paper.

$$\Xi_w(\xi) = \frac{1}{N}\sum_{i=1}^{N} I_{\xi\ge\hat{\xi}_{wi}}, I_{\xi\ge\hat{\xi}_{wi}} = \begin{cases} 1\ \xi \ge \hat{\xi}_{wi} \\ 0\ \text{Otherwise} \end{cases} \tag{61}$$

Moreover, the equation (61) is equivalent to the following linearized formulation:

$$\Xi_w(\xi) = \frac{1}{N}\sum_{i=1}^{N} q_{wi} \tag{62}$$

Subject to

$$q_{wi}\left(\xi - \hat{\xi}_{wi}\right) \ge 0, 0 \le q_{wi} \le 1 \tag{63}$$

Equation (59) needs to be further simplified with the removal of the maximization operator. Based on the Slater condition, the optimality conditions are required to support the outer '*max*' problem. Accordingly, the optimality conditions of $\Xi_w(\xi)$ consist of both the primal and dual constraints with the strong duality characteristic. Thus, constraint (68) becomes:

$$\theta_i + \tau_i \ge \max_{\xi,q_{wim},\delta_{wim},} \Xi(x,\xi_m) - \kappa_i'\left(\hat{\xi}_i - \xi_m\right) - \varsigma_i'\left(\Xi_w\left(\hat{\xi}_i\right) - \frac{1}{N}\begin{pmatrix} \sum_{w=1}^{N} q_{1im} \\ \dots \\ \dots \\ \sum_{w=1}^{N} q_{Wim} \end{pmatrix}\right) \tag{64}$$

Subject to

$$q_{mwi}\left(\xi_w - \hat{\xi}_{wm}\right) \ge 0 \tag{65}$$

$$0 \le q_{mwi} \le 1 \tag{66}$$

$$\frac{1}{N} + \chi_{wmi}\left(\xi_w - \hat{\xi}_{wm}\right) - \vartheta_{wmi} \le 0 \tag{67}$$

Constraint (65) contains bilinear terms, which are relaxed by the McCormick relaxation approach [66, 67]. The tight relaxation can be obtained with the available support set of

$\xi_w \in [\xi_w^{min}, \xi_w^{max}]$. The linearized McCormick reformulation is given:

$$\theta_i + \tau_i \geq \max_{\xi, q_{wim}, \delta_{wim}, \chi_{wim}} \Xi(x, \xi_m) - \kappa_i' \left(\hat{\xi}_i - \xi_m\right) - \varsigma_i' \left(\Xi_w(\hat{\xi}_i) - \frac{1}{N} \begin{pmatrix} \sum_{w=1}^{N} q_{1im} \\ \dots \\ \dots \\ \sum_{w=1}^{N} q_{Wim} \end{pmatrix} \right) \quad (68)$$

$$\alpha_{mwi}^{M} \geq q_{mwi} \hat{\xi}_{wm} \quad : \quad \psi_{wmi}^{(1)} \quad (69)$$

$$\alpha_{mwi}^{M} \geq q_{mwi} \xi_w^{min} \quad : \quad \psi_{wmi}^{(2)} \quad (70)$$

$$\alpha_{mwi}^{M} \geq q_{mwi} \xi_w^{max} : \quad \psi_{wmi}^{(3)} \quad (71)$$

$$\alpha_{mwi}^{M} - q_{mwi} \xi_w^{max} \geq \xi_w - \xi_w^{max} : \quad \psi_{wmi}^{(4)} \quad (72)$$

$$\alpha_{mwi}^{M} - q_{mwi} \xi_w^{min} \geq \xi_w - \xi_w^{min} : \quad \psi_{wmi}^{(5)} \quad (73)$$

$$0 \leq q_{mwi} \leq 1 : \quad \psi_{wmi}^{(6)} \quad (74)$$

Another dualization is required to resolve the *'max'* problem in (69). Therefore, the dual form of equations (68-74) is given as:

$$\min_{\zeta, \nu \geq 0, \theta_i, \tau_i, \chi_m} \zeta \, \eta + \nu \gamma + \frac{1}{N} \sum_{i=1}^{N} \theta_i + \frac{1}{N} \sum_{i=1}^{N} \tau_i \quad (75)$$

Subject to

$$\theta_i \geq b(x) - \kappa_i' \, \hat{\xi}_i - \varsigma_i' \Xi_w(\hat{\xi}_i) + \sum_{w=1}^{W} \sum_{m=1}^{M} \left(\psi_{wmi}^{(3)} \xi_w^{max} - \psi_{wmi}^{(4)} \xi_w^{min} + \psi_{wmi}^{(6)} \right) \quad (76)$$

$$a_w(x) + \kappa_{iw}' + \sum_{w=1}^{W} \sum_{m=1}^{M} \left(\psi_{wmi}^{(3)} + \psi_{wmi}^{(4)} \right) = 0 \quad (77)$$

$$\frac{1}{N} \psi_{wmi}^{(2)} - \psi_{wmi}^{(1)} \hat{\xi}_{wm} - \psi_{wmi}^{(2)} \xi_w^{min} - \psi_{wmi}^{(3)} \xi_w^{max} + \psi_{wmi}^{(4)} \xi_w^{min} + \psi_{wmi}^{(5)} \xi_w^{max} - \psi_{wmi}^{(6)} = 0 \quad (78)$$

$$\psi_{wmi}^{(1)} + \psi_{wmi}^{(2)} + \psi_{wmi}^{(3)} + \psi_{wmi}^{(4)} - \psi_{wmi}^{(5)} - \psi_{wmi}^{(6)} = 0 \quad (79)$$

$$\|\kappa_i\|_* \leq \zeta, \|\varsigma_i\|_* \leq \nu \quad (80)$$

Finally, we have eliminated the *min-max* structure based on the original two-stage formulation (34)-(35). Problem (75)-(80) is a tractable formulation of (53)-(55), which can be solved by an off-the-shelf optimization commercial solver.

C. Approximation of Chance Constraints

We apply the CVaR-based distributionally robust chance constrained (DRCC) approach for realizing chance constraints in (30). The DRCC formulation is given as:

$$\min_{\mathbb{P} \in P_0(\mathbb{R}^{|S|})} \mathbb{P}(c \leq 0) \geq 1 - \epsilon \quad (81)$$

The CVaR approximation for (81) is given in (82) and (83), where π is the auxiliary variable.

$$\max_{\mathbb{P} \in P_0(\mathbb{R}^{|S|})} \mathbb{P}: \mathrm{CVaR}_{\epsilon}(c) \leq 0 \quad (82)$$

$$\min_{\pi \in \mathbb{R}} \pi + \frac{1}{\epsilon} \max_{\mathbb{P} \in P_0(\mathbb{R}^{|S|})} E_{\mathbb{P}}[(c - \pi)^+] \quad (83)$$

The explicit reformulation of (83) is based on [68] recasting the 'max' problem into 'min' problem. The reformulated DRCC problem can be incorporated into the (34)-(80) according to [68].

IV. Case Studies

A. Simulation Setup

To demonstrate the proposed method's effectiveness and practical values, we conducted a total of six case studies with a water-energy system that involves 4 networked WEHs. The structure of a WEH system is given in Fig. 2; as shown, each WEH is composed of PV generators, converters, and storage [69]. The initial load profile can be found in Fig. 10 [70, 71]. The parameters trading amount is summarized in TABLE II [30, 71]. The PV generation and load profile are estimated with a long short-term memory recurrent neural network [72, 73], using the hourly data from the SoLa BRISTOL project in Bath and Bristol, United Kingdom [74, 75]. This project aims to design a smart energy usage pattern for both general consumers and distribution systems, which can increase energy efficiency, reduce energy bills, solve essential network harmonics issues, phase distortions, and improve voltage controls. The root mean square error of the forecasting result is 4.73. Fig. 7 shows a 365-day PV generation data. Fig. 8 demonstrates the copula between the historical and candidate PV generation samples. We solve the proposed water-energy transactive management problem using the YALMIP R20200930 combined with MOSEK version 10 in the MATLAB environment. All the numerical tests were evaluated on a personal computer. The following 6 cases were studied to investigate the impact of PV capacity, trading unit cost and converter capacity on the performance of the proposed model:

Case 1: Baseline case.
Case 2: Considering twice the PV capacity of case 1.
Case 3: Considering twice the trading cost with external markets.
Case 4: Considering twice the P2P trading cost.
Case 5: Considering twice the GSHP capacity.
Case 6: Considering twice the CHP capacity.

TABLE I
TRADING PARAMETERS

Limit	P_{max}^{h2g}	P_{max}^{g2h}	G_{max}^{g2h}	σ_{max}^{g2h}	P_{max}^{h2h}	θ_{max}^{h2h}	$\sigma_{p,max}^{h2h}$
Max	600kWh	400kWh	500kWh	5m^3	500kWh	200kWh	5m^3

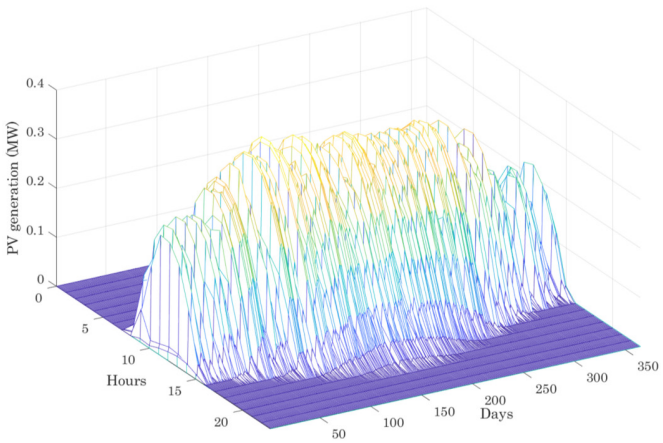

Fig. 7. PV generation profile.

B. Economic Performance Analysis

TABLE II presents the operation costs in each investigated case. Case 1 incurs a cost of $2789 in the first stage and $805 in the second stage. Case 2 attains the lowest operation cost. Its second-stage cost is 8% higher than that of Case 1, partially

since the larger PV capacity not only allows a higher power supply from the WEH itself but also creates higher output deviations. Regardless, the operation cost is still \$734 lower than Case 1. Case 3 has the highest total operation cost, due to the doubled trading cost of external market purchases. The operation costs of the day-ahead and real-time operations are \$5578 and \$912, respectively. A doubled P2P trading cost is applied in Case 4, which has a marginal impact on the day-ahead operations but leads to a total cost 28% higher than that of Case 1. Cases 5 and 6 consider twice the capacity of GSHP and CHP, respectively. Case 5 exhibits a lower operation cost when a higher GSHP capacity is considered, in comparison with Case 6. The conversion efficiency of GSHP is 300%, which results in a lower power consumption but a greater heat output that is doubled in capacity.

TABLE III summarizes the water consumption of CHP, P2G, and electric boiler. As shown, CHP consumes most water in all the investigated cases. Case 1 (i.e., baseline) consumes 51.51 m^3 of water, with CHP accounting for 64% of the water consumption. In Case 2, the water consumed by P2G and electric boiler increase by 34% and 20% from the baseline case. Its PV capacity is doubled, which allows more power supply. Cases 3 and 4 show similar water consumptions relative to Case 1, suggesting an insignificant impact of the trading cost on water consumption. Case 5 takes 42.89 m^3 of water, which is 83% of the consumption in Case 1, partly because GSHP is utilized more frequently without consuming additional water. Yet, the utilization of CHP, P2G, and electric boiler is reduced. In Case 6, 5.8 m^3 more water is consumed when considering twice the capacity of CHP. The total water consumption in Case 6 also increases, reaching 58.22 m^3.

The storage scheduling of WEH 1 in Case 1 is presented in Fig. 9. As shown, the battery is charging before 5:00, followed by a discharging until 8:00 at the lowest capacity level (40kWh). As PV generation increases, the battery remains at full capacity from 11:00 to 15:00. Then, the increasing load in the evening requires another discharging of the battery storage. Heat storage exhibits a pattern similar to that of battery storage, though the highest capacity level (i.e., 90kWh) lasts for two hours only. Overall, the water storage displays general charging before 18:00, followed by a discharging scheduling in the peak load time periods for power, heat, and water. Notably, the extensive usage of energy converters consumes a large amount of water too.

C. *Demand Response Analysis*

Fig. 10 depict the impact of demand response on WEHs. The power load profile under different demand response levels (DRLs) is displayed in Fig. 10 (a), showing that the original peak load at 19:00 is shifted to the morning. As DRL increases, a greater portion of power load in the original high-level load periods is shifted; specifically, the peak load at 19:00 is 378kW when DRL is 30% but 486kW when DRL is 10%. Similarly, both heat and water loads exhibit greater load shifts when DRL increases. Fig. 11 illustrates the total load shift when DRL equals to 10%, 20%, and 30%, respectively. For example, with DRL being 10%, the total load shift of power, heat, and water is 4149kWh, 2800kWh, and 19 m^3, respectively. When DRL is 20%, the load shift increases by 175% for power, 187% for heat, and 163% for water. With DRL equal to 30%, the increases in power, heat, and water load shifts attenuate, with the power load shift greater than that of heat or water.

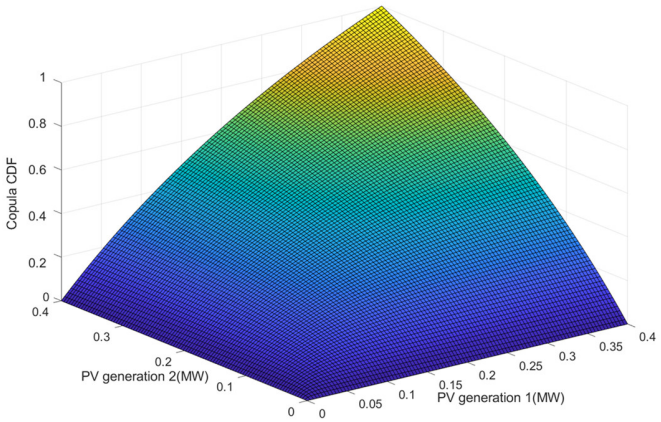

Fig. 8. Copula cumulative distribution function of two sets of PV generation output.

TABLE II
ECONOMIC PERFORMANCE FOR ALL CASES

Economic result (\$)	Case 1	Case 2	Case 3	Case 4	Case 5	Case 6
First-stage cost	2789	1986	5578	2780	2042	2529
Expected second-stage cost	805	874	912	1033	840	852
Total cost	3594	2860	6490	3813	2882	3381

TABLE III
WATER CONSUMPTION BY CONVERTERS

Water (m^3)	Case 1	Case 2	Case 3	Case 4	Case 5	Case 6
CHP	33.30	30.03	33.32	33.32	28.68	39.10
P2G	5.34	7.19	5.69	5.47	4.15	4.60
Boiler	12.87	15.44	13.50	13.02	10.06	14.52
Total	51.51	52.66	52.51	51.81	42.89	58.22

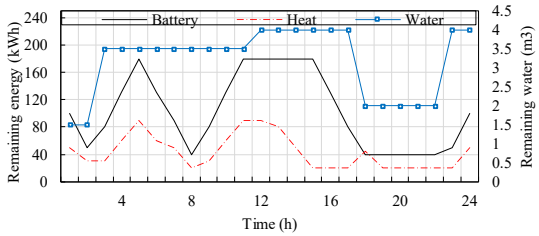

Fig. 9. Remaining energy and water storage under case 1.

D. *Blockchain-Based P2P Trading Analysis*

In this paper, we employ the P2P trading as an effective measure to realize decentralized management and improve the system efficiency of the entire WEH community. The effectiveness of employing P2P trading can be reflected in TABLE II, TABLE IV, and Fig. 12 which directly demonstrate the P2P trading amount. TABLE IV summarizes the volume of power, heat, and water trading via P2P. Case 1 has 24500kWh, 10219kWh, and 265 m^3 in power, heat, and water trading, respectively. With the twice capacity of PV, Case 2 records higher power and heat trading. Case 3 features a doubled trading cost with external markets, which elevates P2P trading; i.e., 2010kWh for power, 1981kWh for heat, and 16 m^3 for

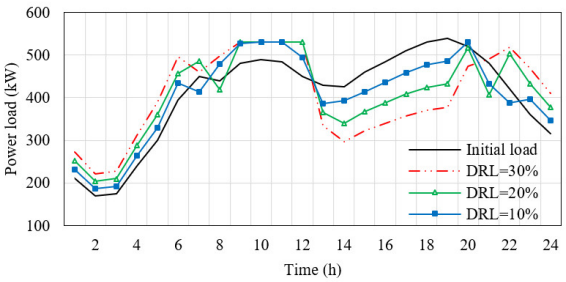

(a) power load

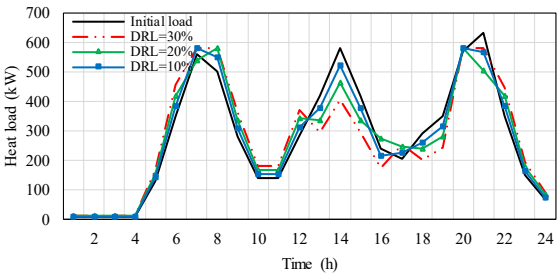

(b) heat load

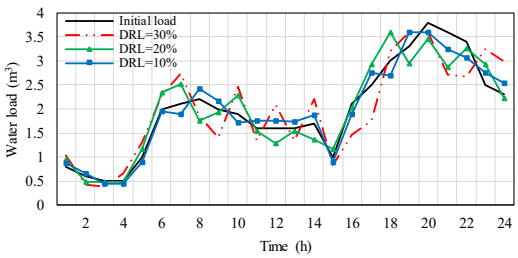

(c) water load

Fig. 10. Altered load applying DRLs.

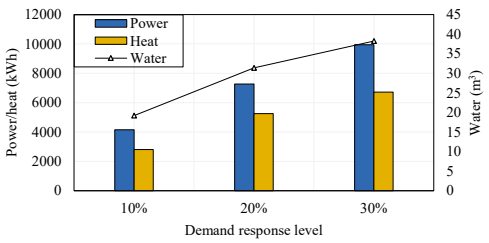

Fig. 11. Total altered load profile under different DRLs.

water. In contrast, Case 4 shows less P2P trading, mainly because the trading unit cost is now doubled. To illustrate, the power trading is only 85% of that in Case 1. Case 5 has less power trading but more heat trading, probably because the greater GSHP capacity leads to an increased power-to-heat conversion and therefore reduces the (total) operation costs. Meanwhile, the water trading drops by 48 m^3, as the converters that consumes water are used at a lower level.

Fig. 12 shows the P2P trading scheduling. As shown in Fig. 12 (a), WEH 4 mainly purchases power and WEHs 1–3 instead sell power primarily. There are multiple trading peaks (400kW) in the entire time horizon. Relatively, heat P2P trading features more frequent P2P transactions, with consistent trading at the highest level except 1:00–4:00 and 15:00–18:00 (see Fig. 12 (b)). There are no direct buying heat from the market, so either P2P heat purchases or power-to-heat and gas-to-heat

TABLE IV
P2P TRADING AMOUNT

Trading amount	Case 1	Case 2	Case 3	Case 4	Case 5	Case 6
Power (kWh)	24500	25198	26510	20986	22100	24008
Heat (kWh)	10219	10414	12200	9214	10328	9803
Water (m^3)	265	269	281	217	259	277

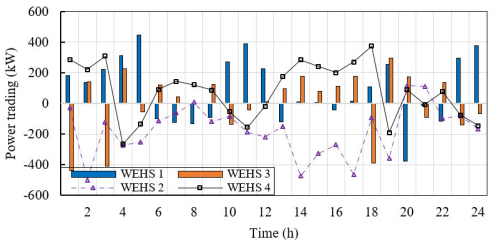

(a) power trading

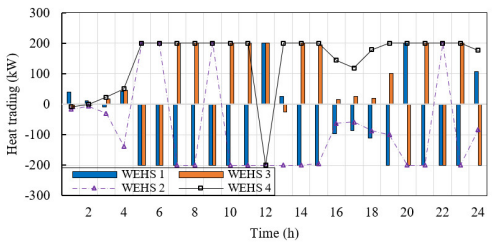

(b) heat trading

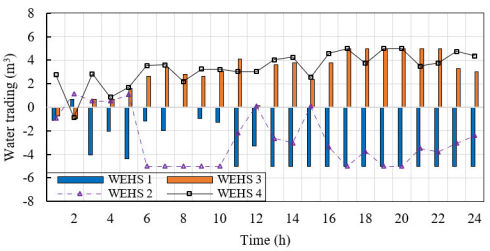

(c) water trading

Fig. 12. P2P trading scheduling of power, heat, and water.

conversions take place during the high demand periods for heat. Energy conversions inevitably cause energy losses, which favors more active heat P2P trading than power P2P trading. Fig. 12 (c) details the water P2P trading patterns with multiple trading peaks.

E. Comparative Analysis

We then compare the proposed two-stage blockchain-based spatial-temporal transactive management framework (TS-STDRO) with the existing frameworks including a single-stage robust optimization [15] and a two-stage moment-based DRO [41, 42], which are denoted as SS and TS-MDRO. In Fig. 13, we compare the second-stage expected operation cost results between TS-MDRO and TS-STDRO. The PoX and trading deviation penalty cost coefficients are adjusted and the results suggest that a monotone increasing trend of the operation cost. Overall, the results of TS-MDRO are generally higher than that of the proposed TS-STDRO, which peak at \$1416 and \$1326, respectively.

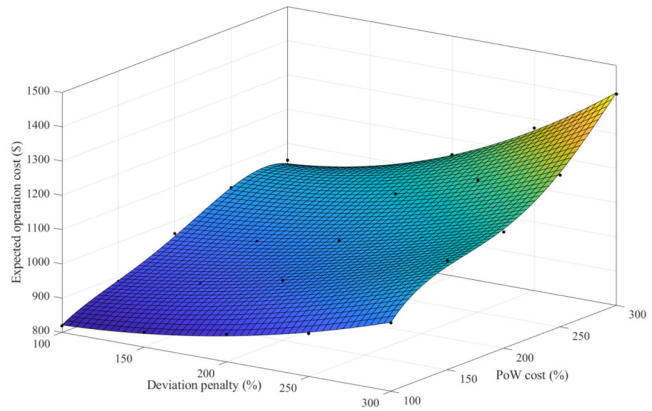

(a) TS-MDRO

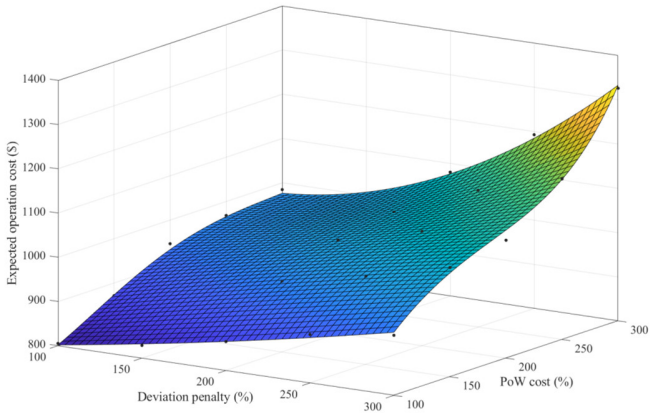

(b) TS-STDRO

Fig. 13. Expected second-stage operation costs of TS-MDRO and TS-STDRO.

In TABLE V, we compare the total operation cost results between the three different methods, which demonstrates that the proposed TS-STDRO is able to reduce the computational conservativeness with the lowest operation cost among cases 1-4. TS-STDRO is economically effective in reducing 2.3% and 6.1% of the operation cost compared with TS-MDRO and SS. Moreover, the results of power and water trading amount are given in Fig. 14. Both the left and right panels show that the trading amount decreases with the growth of PoX cost coefficient. Instead of implementing P2P trading with other WEHs, the WEH owners choose to trade more with the MGO. The comparative analyses reveal that TS-STDRO can produce a scheme that features higher P2P trading volumes than that by any benchmark, because it can better characterize the associated uncertainties. Overall, the evaluation results suggest that our method is practical and enables effective water-energy transactive management, with the assumption of moderate fluctuations in renewable generation and load.

We empirically examine the computational efficiency of each method. In Fig. 15, TS-MDRO has the most stringent run time, which is an averagely 3894 seconds when the sample size is 1000. An iterative constraint and column generation algorithm is applied to search for the optimality within upper and lower bounds. The proposed TS-STDRO shows higher computational efficiency. We test the performance when γ is 0.05 and 0.1, respectively. The computational time are 2937 and 3124 seconds. It shows that the result with γ=0.05 is more efficient due to the smaller copula radius of the ambiguity set. The tighter ambiguity set has a relatively smaller feasibility area with reduced computational complexity.

TABLE V
THE OPERATION COST COMPARISON ($)

Methods	Case 1	Case 2	Case 3	Case 4
SS	3782	3014	6990	4112
TS-MDRO	3670	2899	6712	3903
TS-STDRO	3594	2860	6490	3813

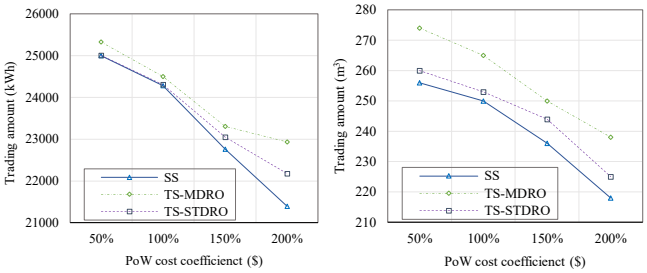

Fig. 14. Comparison with the benchmark on trading amount.

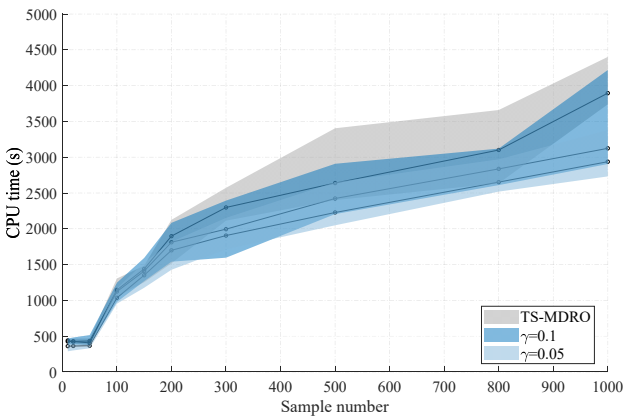

Fig. 15. Computational time comparison of TS-MDRO and TS-STDRO with γ=0.1 and γ =0.05.

F. *Discussions*

Incorporating TS-STDRO in the proposed blockchain-based WEH trading mechanism is valuable and cost-effective. In Section E, we compare TS-STDRO and the state-of-the-art TS-MDRO. As shown, the proposed TS-STDRO method achieves an average 4.6% reduction in total operation cost than TS-MDRO, across all deviation penalties and PoX cost conditions. TABLE V reveals the desirable cost reduction by TS-STDRO, which is economically effective and capable of decreasing the operation cost by 2.3% and 6.1% relative to TS-MDRO and SS, respectively. These comparative results demonstrate that TS-STDRO is more cost-effective than the commonly used RO, an extreme uncertainty modelling method with enormous, inherent conservativeness [45, 76]. Jointly, our evaluation results

indicate that TS-STDRO outperforms existing blockchain-based trading mechanisms in cost effectiveness [77, 78].

This study can inform the practicability for related research. The proposed WEH is a hypothetical term to define the community-scale hybrid water-energy systems, which contains: i) the energy vectors of power, natural gas, water, and heating; ii) the interdependencies between water and energy; iii) energy converters of electricity generation, P2G, gas furnace, boiler, CHP, GSHP, renewable energy (PV); iv) storage devices of battery, water, and heat. In particular, the energy converters can efficiently satisfy energy demand through conversion between energy vectors. The proposed WEH system is suitable for small-scale buildings, such as residential buildings, hospitals, and shopping malls. The capacity of PV, converters and ESS are all appropriate for small-scale buildings at the community level. Moreover, we believe that the proposed two-stage framework can produce a more practical scheme for WEH owners to prepare operations and transactions in the first 24 hours, then adjust the prespecified plan in the next day.

This paper adopts the real-world energy and water prosumer data based on the SoLa BRISTOL project [74, 75] in the United Kingdom, which was practiced in energy communities. When considering a specific WEH into practice, more factors should be considered. For example, the energy and water losses, which have unignorable impacts on operational efficiency and economic benefits. In addition, other uncertainties such as trading willingness of prosumers, water and energy prices should be modelled, which can also be handled by the proposed TS-STDRO approach with more explicit data.

V. Conclusion

This study develops an innovative, blockchain-based water-energy hub operation scheme that offers optimality, security, and transparency in the water-energy nexus for multi-energy systems. Optimal coordination and complementation via energy converters are central to the economic efficiency and safety of WEH operations. In that regard, we design a blockchain-based P2P trading mechanism for interconnected WEHs to trade surplus energy that pertains to power, heat, and water for increased economic efficiency. Additionally, we leverage a consensus-based trading mechanism to audit and encrypt transaction records that are stored in a consortium blockchain. The spatial-temporal ambiguity set in DRO can handle uncertainties effectively by characterizing PV uncertainties with a tractable robust counterpart reformulation. Moreover, the proposed two-stage trading method benefits both WEH operators and external markets by allowing greater flexibility and a more effective, preparatory plan in the day-ahead stage. It allows trading between external water and energy markets in the day-ahead stage. In the second (real-time) stage, corrective operations can be made to properly adjust trading and converter scheduling in which demand response and blockchain-based P2P trading resemble real-time scenarios. Six case studies are performed and the results demonstrate the effectiveness of our two-stage transactive management method which allows WEH operators to formulate practical, economical, and secure operation plans for the entire WEH system that is crucial to the water-energy nexus. Key findings derived from the simulation study imply that:

i) Early investment on PV installation could result in 20% saving of the WEH operation cost.

ii) Meanwhile, on the contrary, the twice of PV capacity expectedly causes 8% higher cost in the second-stage adjustment.

iii) Therefore, the proposed TS-STDRO is designed to effectively handle the inherent system uncertainties, which yields 2.3% and 6.1% compared with the state-of-the-art SS and TS-MDRO methods.

iv) Moreover, the proposed TS-STDRO is computationally efficient. In particular, it reduces 18.7% of the computational time compared with the prevalent TS-MDRO.

v) Enhanced by the proposed two-stage blockchain-based trading mechanism, the trading security is ensured.

Two directions are important and deserve further investigative efforts. First, auction-based P2P trading mechanisms are essential and promising for the increased social welfare of prosumers. Future research can extend our method by considering these trading mechanisms. Second, the proposed blockchain-based transactive management scheme can be enhanced with advanced encryption and auditing, as well as appropriate success rate modelling.

References

[1] C. Tan and Q. Zhi, "The energy-water nexus: A literature review of the dependence of energy on water," *Energy Procedia,* vol. 88, pp. 277-284, 2016.

[2] S. Lu, W. Gu, S. Ding, S. Yao, H. Lu, and X. Yuan, "Data-Driven Aggregate Thermal Dynamic Model for Buildings: A Regression Approach," *IEEE Transactions on Smart Grid,* vol. 13, no. 1, pp. 227-242, 2022, doi: 10.1109/TSG.2021.3101357.

[3] P. Zhao *et al.*, "Water-Energy Nexus Management for Power Systems," *IEEE Transactions on Power Systems,* vol. 36, no. 3, pp. 2542-2554, 2021, doi: 10.1109/TPWRS.2020.3038076.

[4] S. Chen, A. J. Conejo, and Z. Wei, "Conjectural-Variations Equilibria in Electricity, Natural-Gas, and Carbon-Emission Markets," *IEEE Transactions on Power Systems,* vol. 36, no. 5, pp. 4161-4171, 2021, doi: 10.1109/TPWRS.2021.3066459.

[5] Z. Li, L. Wu, Y. Xu, and X. Zheng, "Stochastic-Weighted Robust Optimization Based Bilayer Operation of a Multi-Energy Building Microgrid Considering Practical Thermal Loads and Battery Degradation," *IEEE Transactions on Sustainable Energy,* vol. 13, no. 2, pp. 668-682, 2022, doi: 10.1109/TSTE.2021.3126776.

[6] J. Hu, X. Liu, M. Shahidehpour, and S. Xia, "Optimal Operation of Energy Hubs With Large-Scale Distributed Energy Resources for Distribution Network Congestion Management," *IEEE Transactions on Sustainable Energy,* vol. 12, no. 3, pp. 1755-1765, 2021, doi: 10.1109/TSTE.2021.3064375.

[7] P. Zhao, C. Gu, D. Huo, Y. Shen, and I. Hernando-Gil, "Two-Stage Distributionally Robust Optimization for Energy Hub Systems," *IEEE Transactions on Industrial Informatics,* vol. 16, no. 5, pp. 3460-3469, 2020, doi: 10.1109/TII.2019.2938444.

[8] N. Gu, J. Cui, and C. Wu, "Power-Electronics-Enabled Transactive Energy Market Design for Distribution Networks," *IEEE Transactions on Smart Grid,* pp. 1-1, 2021, doi: 10.1109/TSG.2021.3127544.

[9] M. Montakhabi, A. Madhusudan, S. Van Der Graaf, A. Abidin, P. Ballon, and M. A. Mustafa, "Sharing economy in future peer-to-peer electricity trading markets: Security and privacy analysis," in *Proceedings of the Workshop on Decentralized IoT Systems and Security (DISS), San Diego, CA, USA*, 2020, pp. 1-6.

[10] A. K. Tiwari, S. Kumar, and R. Pathak, "Modelling the dynamics of Bitcoin and Litecoin: GARCH versus stochastic volatility models," *Applied Economics,* vol. 51, no. 37, pp. 4073-4082, 2019.

[11] J. Abdella, Z. Tari, A. Anwar, A. Mahmood, and F. Han, "An Architecture and Performance Evaluation of Blockchain-Based Peer-to-Peer Energy Trading," *IEEE Transactions on Smart Grid,* vol. 12, no. 4, pp. 3364-3378, 2021, doi: 10.1109/TSG.2021.3056147.

[12] M. K. AlAshery *et al.*, "A Blockchain-Enabled Multi-Settlement Quasi-Ideal Peer-to-Peer Trading Framework," *IEEE Transactions on Smart Grid,* vol. 12, no. 1, pp. 885-896, 2021, doi: 10.1109/TSG.2020.3022601.
[13] V. Gramoli, "From blockchain consensus back to Byzantine consensus," *Future Generation Computer Systems,* vol. 107, pp. 760-769, 2020.
[14] L. M. Bach, B. Mihaljevic, and M. Zagar, "Comparative analysis of blockchain consensus algorithms," in *2018 41st International Convention on Information and Communication Technology, Electronics and Microelectronics (MIPRO)*, 2018: IEEE, pp. 1545-1550.
[15] Z. Li, Y. Xu, S. Fang, X. Zheng, and X. Feng, "Robust Coordination of a Hybrid AC/DC Multi-Energy Ship Microgrid With Flexible Voyage and Thermal Loads," *IEEE Transactions on Smart Grid,* vol. 11, no. 4, pp. 2782-2793, 2020, doi: 10.1109/TSG.2020.2964831.
[16] F. Zhu, J. Fu, P. Zhao, and D. Xie, "Robust energy hub optimization with cross-vector demand response," *International Transactions on Electrical Energy Systems,* https://doi.org/10.1002/2050-7038.12559 vol. 30, no. 10, p. e12559, 2020/10/01 2020, doi: https://doi.org/10.1002/2050-7038.12559.
[17] Q. Zhang, Z. Wang, S. Ma, and A. Arif, "Stochastic pre-event preparation for enhancing resilience of distribution systems," *Renewable and Sustainable Energy Reviews,* vol. 152, p. 111636, 2021/12/01/ 2021, doi: https://doi.org/10.1016/j.rser.2021.111636.
[18] X. Xu, J. Li, Z. Xu, J. Zhao, and C. S. Lai, "Enhancing photovoltaic hosting capacity—A stochastic approach to optimal planning of static var compensator devices in distribution networks," *Applied Energy,* vol. 238, pp. 952-962, 2019/03/15/ 2019, doi: https://doi.org/10.1016/j.apenergy.2019.01.135.
[19] S. Lu, W. Gu, K. Meng, and Z. Dong, "Economic Dispatch of Integrated Energy Systems With Robust Thermal Comfort Management," *IEEE Transactions on Sustainable Energy,* vol. 12, no. 1, pp. 222-233, 2021, doi: 10.1109/TSTE.2020.2989793.
[20] P. Zhao, C. Gu, and D. Huo, "Coordinated Risk Mitigation Strategy For Integrated Energy Systems Under Cyber-Attacks," *IEEE Transactions on Power Systems,* vol. 35, no. 5, pp. 4014-4025, 2020, doi: 10.1109/TPWRS.2020.2986455.
[21] D. Bertsimas, M. Sim, and M. Zhang, "Adaptive Distributionally Robust Optimization," *Management Science,* vol. 65, no. 2, pp. 604-618, 2019/02/01 2018, doi: 10.1287/mnsc.2017.2952.
[22] X. Lu *et al.*, "A Real-Time Alternating Direction Method of Multipliers Algorithm for Nonconvex Optimal Power Flow Problem," *IEEE Transactions on Industry Applications,* vol. 57, no. 1, pp. 70-82, 2021, doi: 10.1109/TIA.2020.3029549.
[23] C. Wang, R. Gao, W. Wei, M. Shafie-khah, T. Bi, and J. P. S. Catalão, "Risk-Based Distributionally Robust Optimal Gas-Power Flow With Wasserstein Distance," *IEEE Transactions on Power Systems,* vol. 34, no. 3, pp. 2190-2204, 2019, doi: 10.1109/TPWRS.2018.2889942.
[24] K. Oikonomou and M. Parvania, "Optimal Coordinated Operation of Interdependent Power and Water Distribution Systems," *IEEE Transactions on Smart Grid,* vol. 11, no. 6, pp. 4784-4794, 2020, doi: 10.1109/TSG.2020.3000173.
[25] Q. Li, S. Yu, A. S. Al-Sumaiti, and K. Turitsyn, "Micro Water–Energy Nexus: Optimal Demand-Side Management and Quasi-Convex Hull Relaxation," *IEEE Transactions on Control of Network Systems,* vol. 6, no. 4, pp. 1313-1322, 2019, doi: 10.1109/TCNS.2018.2889001.
[26] H. Mehrjerdi, "Modeling and optimization of an island water-energy nexus powered by a hybrid solar-wind renewable system," *Energy,* vol. 197, p. 117217, 2020/04/15/ 2020, doi: https://doi.org/10.1016/j.energy.2020.117217.
[27] W. Wang, R. Jing, Y. Zhao, C. Zhang, and X. Wang, "A load-complementarity combined flexible clustering approach for large-scale urban energy-water nexus optimization," *Applied Energy,* vol. 270, p. 115163, 2020/07/15/ 2020, doi: https://doi.org/10.1016/j.apenergy.2020.115163.
[28] E. Martinez-Cesena *et al.*, "Quantifying the Impacts of Modelling Assumptions on Accuracy and Computational Efficiency for Integrated Water-Energy System Simulations Under Uncertain Climate," *IEEE Transactions on Sustainable Energy,* pp. 1-1, 2022, doi: 10.1109/TSTE.2022.3155073.
[29] S. Zuloaga and V. Vittal, "Integrated Electric Power/Water Distribution System Modeling and Control Under Extreme Mega Drought Scenarios," *IEEE Transactions on Power Systems,* vol. 36, no. 1, pp. 474-484, 2021, doi: 10.1109/TPWRS.2020.3001588.
[30] M. J. Vahid Pakdel, F. Sohrabi, and B. Mohammadi-Ivatloo, "Multi-objective optimization of energy and water management in networked hubs considering transactive energy," *Journal of Cleaner Production,* vol. 266, p. 121936, 2020/09/01/ 2020, doi: https://doi.org/10.1016/j.jclepro.2020.121936.
[31] M. Roustaei *et al.*, "A scenario-based approach for the design of Smart Energy and Water Hub," *Energy,* vol. 195, p. 116931, 2020/03/15/ 2020, doi: https://doi.org/10.1016/j.energy.2020.116931.
[32] R. Ghaffarpour, B. Mozafari, A. M. Ranjbar, and T. Torabi, "Resilience oriented water and energy hub scheduling considering maintenance constraint," *Energy,* vol. 158, pp. 1092-1104, 2018/09/01/ 2018, doi: https://doi.org/10.1016/j.energy.2018.06.022.
[33] X. Huang, Y. Zhang, D. Li, and L. Han, "A Solution for Bi-layer Energy Trading Management in Microgrids Using Multi-Blockchain," *IEEE Internet of Things Journal,* pp. 1-1, 2022, doi: 10.1109/JIOT.2022.3142815.
[34] M. Yan *et al.*, "Blockchain for Transacting Energy and Carbon Allowance in Networked Microgrids," *IEEE Transactions on Smart Grid,* vol. 12, no. 6, pp. 4702-4714, 2021, doi: 10.1109/TSG.2021.3109103.
[35] H. Huang, W. Miao, Z. Li, J. Tian, C. Wang, and G. Min, "Enabling Energy Trading in Cooperative Microgrids: A Scalable Blockchain-based Approach with Redundant Data Exchange," *IEEE Transactions on Industrial Informatics,* pp. 1-1, 2021, doi: 10.1109/TII.2021.3115576.
[36] Q. Yang and H. Wang, "Blockchain-Empowered Socially Optimal Transactive Energy System: Framework and Implementation," *IEEE Transactions on Industrial Informatics,* vol. 17, no. 5, pp. 3122-3132, 2021, doi: 10.1109/TII.2020.3027577.
[37] W. Hua, Y. Zhou, M. Qadrdan, J. Wu, and N. Jenkins, "Blockchain Enabled Decentralized Local Electricity Markets with Flexibility from Heating Sources," *IEEE Transactions on Smart Grid,* pp. 1-1, 2022, doi: 10.1109/TSG.2022.3158732.
[38] H. Abdelsalam, A. Srivastava, and A. Eldosouky, "Blockchain-Based Privacy Preserving and Energy Saving Mechanism for Electricity Prosumers," *IEEE Transactions on Sustainable Energy,* pp. 1-1, 2021, doi: 10.1109/TSTE.2021.3109482.
[39] Y. Xu, Z. Liu, C. Zhang, J. Ren, Y. Zhang, and X. Shen, "Blockchain-based Trustworthy Energy Dispatching Approach for High Renewable Energy Penetrated Power Systems," *IEEE Internet of Things Journal,* pp. 1-1, 2021, doi: 10.1109/JIOT.2021.3117924.
[40] P. Li, M. Yang, and Q. Wu, "Confidence Interval Based Distributionally Robust Real-Time Economic Dispatch Approach Considering Wind Power Accommodation Risk," *IEEE Transactions on Sustainable Energy,* vol. 12, no. 1, pp. 58-69, 2021, doi: 10.1109/TSTE.2020.2978634.
[41] E. Delage and Y. Ye, "Distributionally robust optimization under moment uncertainty with application to data-driven problems," *Operations research,* vol. 58, no. 3, pp. 595-612, 2010.
[42] X. Lu, K. W. Chan, S. Xia, B. Zhou, and X. Luo, "Security-Constrained Multiperiod Economic Dispatch With Renewable Energy Utilizing Distributionally Robust Optimization," *IEEE Transactions on Sustainable Energy,* vol. 10, no. 2, pp. 768-779, 2019, doi: 10.1109/TSTE.2018.2847419.
[43] Y. Chen, Q. Guo, H. Sun, Z. Li, W. Wu, and Z. Li, "A Distributionally Robust Optimization Model for Unit Commitment Based on Kullback–Leibler Divergence," *IEEE Transactions on Power Systems,* vol. 33, no. 5, pp. 5147-5160, 2018, doi: 10.1109/TPWRS.2018.2797069.
[44] A. Arrigo, C. Ordoudis, J. Kazempour, Z. De Grève, J.-F. Toubeau, and F. Vallée, "Wasserstein distributionally robust chance-constrained optimization for energy and reserve dispatch: An exact and physically-bounded formulation," *European Journal of Operational Research,* vol. 296, no. 1, pp. 304-322, 2022.
[45] X. Lu, K. W. Chan, S. Xia, M. Shahidehpour, and W. H. Ng, "An Operation Model for Distribution Companies Using the Flexibility of Electric Vehicle Aggregators," *IEEE Transactions on Smart Grid,* vol. 12, no. 2, pp. 1507-1518, 2021, doi: 10.1109/TSG.2020.3037053.
[46] Y. Ding, T. Morstyn, and M. D. McCulloch, "Distributionally Robust Joint Chance-Constrained Optimization for Networked Microgrids Considering Contingencies and Renewable Uncertainty," *IEEE Transactions on Smart Grid,* vol. 13, no. 3, pp. 2467-2478, 2022, doi: 10.1109/TSG.2022.3150397.
[47] L. Yang, Y. Xu, J. Zhou, and H. Sun, "Distributionally Robust Frequency Constrained Scheduling for an Integrated Electricity-Gas System," *IEEE Transactions on Smart Grid,* pp. 1-1, 2022, doi: 10.1109/TSG.2022.3158942.
[48] Z. Liu and L. Wang, "A Robust Strategy for Leveraging Soft Open Points to Mitigate Load Altering Attacks," *IEEE Transactions on Smart Grid,* vol. 13, no. 2, pp. 1555-1569, 2022, doi: 10.1109/TSG.2021.3134176.
[49] R. Xie, W. Wei, M. Shahidehpour, Q. Wu, and S. Mei, "Sizing Renewable Generation and Energy Storage in Stand-Alone Microgrids Considering Distributionally Robust Shortfall Risk," *IEEE Transactions on Power Systems,* pp. 1-1, 2022, doi: 10.1109/TPWRS.2022.3142006.
[50] J. Li, M. E. Khodayar, J. Wang, and B. Zhou, "Data-Driven Distributionally Robust Co-Optimization of P2P Energy Trading and Network Operation for Interconnected Microgrids," *IEEE Transactions on Smart Grid,* vol. 12, no. 6, pp. 5172-5184, 2021, doi: 10.1109/TSG.2021.3095509.
[51] G. Chen, H. Zhang, H. Hui, and Y. Song, "Fast Wasserstein-Distance-Based Distributionally Robust Chance-Constrained Power Dispatch for Multi-

Zone HVAC Systems," *IEEE Transactions on Smart Grid,* vol. 12, no. 5, pp. 4016-4028, 2021, doi: 10.1109/TSG.2021.3076237.
[52] Z. Chu, N. Zhang, and F. Teng, "Frequency-Constrained Resilient Scheduling of Microgrid: A Distributionally Robust Approach," *IEEE Transactions on Smart Grid,* vol. 12, no. 6, pp. 4914-4925, 2021, doi: 10.1109/TSG.2021.3095363.
[53] Y. Zhou, Z. Wei, M. Shahidehpour, and S. Chen, "Distributionally Robust Resilient Operation of Integrated Energy Systems Using Moment and Wasserstein Metric for Contingencies," *IEEE Transactions on Power Systems,* vol. 36, no. 4, pp. 3574-3584, 2021, doi: 10.1109/TPWRS.2021.3049717.
[54] C. Wang, N. Gao, J. Wang, N. Jia, T. Bi, and K. Martin, "Robust Operation of a Water-Energy Nexus: A Multi-Energy Perspective," *IEEE Transactions on Sustainable Energy,* vol. 11, no. 4, pp. 2698-2712, 2020, doi: 10.1109/TSTE.2020.2971259.
[55] Q. Tan, Y. Liu, and X. Zhang, "Stochastic optimization framework of the energy-water-emissions nexus for regional power system planning considering multiple uncertainty," *Journal of Cleaner Production,* vol. 281, p. 124470, 2021/01/25/ 2021, doi: https://doi.org/10.1016/j.jclepro.2020.124470.
[56] K. Zhang *et al.*, "Multi-objective optimization of energy-water nexus from spatial resource reallocation perspective in China," *Applied Energy,* vol. 314, p. 118919, 2022/05/15/ 2022, doi: https://doi.org/10.1016/j.apenergy.2022.118919.
[57] S. Zuloaga, P. Khatavkar, L. Mays, and V. Vittal, "Resilience of Cyber-Enabled Electrical Energy and Water Distribution Systems Considering Infrastructural Robustness Under Conditions of Limited Water and/or Energy Availability," *IEEE Transactions on Engineering Management,* vol. 69, no. 3, pp. 639-655, 2022, doi: 10.1109/TEM.2019.2937728.
[58] Y. Wang *et al.*, "Security enhancement technologies for smart contracts in the blockchain: A survey," *Transactions on Emerging Telecommunications Technologies,* https://doi.org/10.1002/ett.4341 vol. 32, no. 12, p. e4341, 2021/12/01 2021, doi: https://doi.org/10.1002/ett.4341.
[59] X. Chen and X. Zhang, "Secure Electricity Trading and Incentive Contract Model for Electric Vehicle Based on Energy Blockchain," *IEEE Access,* vol. 7, pp. 178763-178778, 2019, doi: 10.1109/ACCESS.2019.2958122.
[60] E. K. Wang, R. Sun, C.-M. Chen, Z. Liang, S. Kumari, and M. K. Khan, "Proof of X-repute blockchain consensus protocol for IoT systems," *Computers & Security,* vol. 95, p. 101871, 2020.
[61] F. Saleh, "Blockchain without waste: Proof-of-stake," *The Review of financial studies,* vol. 34, no. 3, pp. 1156-1190, 2021.
[62] D. Zhang, H. Zhu, H. Zhang, H. H. Goh, H. Liu, and T. Wu, "Multi-Objective Optimization for Smart Integrated Energy System Considering Demand Responses and Dynamic Prices," *IEEE Transactions on Smart Grid,* vol. 13, no. 2, pp. 1100-1112, 2022, doi: 10.1109/TSG.2021.3128547.
[63] S. Zheng *et al.*, "Incentive-Based Integrated Demand Response for Multiple Energy Carriers Considering Behavioral Coupling Effect of Consumers," *IEEE Transactions on Smart Grid,* vol. 11, no. 4, pp. 3231-3245, 2020, doi: 10.1109/TSG.2020.2977093.
[64] H. Shareef, M. S. Ahmed, A. Mohamed, and E. A. Hassan, "Review on Home Energy Management System Considering Demand Responses, Smart Technologies, and Intelligent Controllers," *IEEE Access,* vol. 6, pp. 24498-24509, 2018, doi: 10.1109/ACCESS.2018.2831917.
[65] T. Samad, E. Koch, and P. Stluka, "Automated Demand Response for Smart Buildings and Microgrids: The State of the Practice and Research Challenges," *Proceedings of the IEEE,* vol. 104, no. 4, pp. 726-744, 2016, doi: 10.1109/JPROC.2016.2520639.
[66] P. M. Castro, "Tightening piecewise McCormick relaxations for bilinear problems," *Computers & Chemical Engineering,* vol. 72, pp. 300-311, 2015.
[67] Y. Zhang, J. Wang, B. Zeng, and Z. Hu, "Chance-constrained two-stage unit commitment under uncertain load and wind power output using bilinear benders decomposition," *IEEE Transactions on Power Systems,* vol. 32, no. 5, pp. 3637-3647, 2017.
[68] P. M. Esfahani and D. Kuhn, "Data-driven distributionally robust optimization using the Wasserstein metric: Performance guarantees and tractable reformulations," *Mathematical Programming,* vol. 171, no. 1-2, pp. 115-166, 2018.
[69] D. Huo, C. Gu, D. Greenwood, Z. Wang, P. Zhao, and J. Li, "Chance-constrained optimization for integrated local energy systems operation considering correlated wind generation," *International Journal of Electrical Power & Energy Systems,* vol. 132, p. 107153, 2021/11/01/ 2021, doi: https://doi.org/10.1016/j.ijepes.2021.107153.
[70] M. Herrera, L. Torgo, J. Izquierdo, and R. Pérez-García, "Predictive models for forecasting hourly urban water demand," *Journal of Hydrology,* vol. 387, no. 1, pp. 141-150, 2010/06/07/ 2010, doi: https://doi.org/10.1016/j.jhydrol.2010.04.005.
[71] D. Huo, C. Gu, K. Ma, W. Wei, Y. Xiang, and S. L. Blond, "Chance-Constrained Optimization for Multienergy Hub Systems in a Smart City," *IEEE Transactions on Industrial Electronics,* vol. 66, no. 2, pp. 1402-1412, 2019, doi: 10.1109/TIE.2018.2863197.
[72] S. Li, P. Zhao, C. Gu, J. Li, S. Cheng, and M. Xu, "Online Battery Protective Energy Management for Energy-Transportation Nexus," *IEEE Transactions on Industrial Informatics,* pp. 1-1, 2022, doi: 10.1109/TII.2022.3163778.
[73] S. Li *et al.*, "Online battery-protective vehicle to grid behavior management," *Energy,* vol. 243, p. 123083, 2022/03/15/ 2022, doi: https://doi.org/10.1016/j.energy.2021.123083.
[74] W. P. Distribution, "SoLa Bristol SDRC 9.8 Final Report," *Western Power Distribution: Bristol, UK,* 2016.
[75] N. Dale, R. Hey, and P. Swift, "Project sola bristol closedown report western power distribution," ed: Accessed: Mar, 2019.
[76] P. Zhao *et al.*, "Cyber-Resilient Multi-Energy Management for Complex Systems," *IEEE Transactions on Industrial Informatics,* vol. 18, no. 3, pp. 2144-2159, 2022, doi: 10.1109/TII.2021.3097760.
[77] M. Dabbaghjamanesh, B. Wang, A. Kavousi-Fard, N. D. Hatziargyriou, and J. Zhang, "Blockchain-Based Stochastic Energy Management of Interconnected Microgrids Considering Incentive Price," *IEEE Transactions on Control of Network Systems,* vol. 8, no. 3, pp. 1201-1211, 2021, doi: 10.1109/TCNS.2021.3059851.
[78] S. Cui, Y. W. Wang, C. Li, and J. W. Xiao, "Prosumer Community: A Risk Aversion Energy Sharing Model," *IEEE Transactions on Sustainable Energy,* vol. 11, no. 2, pp. 828-838, 2020, doi: 10.1109/TSTE.2019.2909301.

Pengfei Zhao was born in Beijing, China. He received the double B.Eng. degree from the University of Bath, U.K., and North China Electric Power University, Baoding, China, in 2017. He received the Ph.D degree from the University of Bath, U.K. in 2021. He was a visiting Ph.D. student at Smart Grid Operations and Optimization Laboratory (SGOOL), Tsinghua University, Beijing, China in 2019. Dr. Zhao is currently an Assistant Professor at the State Key Laboratory of Management and Control for Complex Systems, Institute of Automation, Chinese Academy of Sciences, Beijing. His major research interests include the low-carbon energy systems, social computing, complex systems and cyber-physical-social systems.

Shuangqi Li was born in Beijing, China. He received the B.Eng. degree in vehicle engineering from the Beijing Institute of Technology, Beijing, China, in 2018. He is currently pursuing the Ph.D. degree in electrical engineering with the Department of Electronic and Electrical Engineering, University of Bath, Bath, U.K. He was a Research Assistant with the National Engineering Laboratory for Electric Vehicles, Beijing Institute of Technology, Beijing, from 2018 to 2019. Since 2022, he has also been a Visiting Ph.D. Student with the Department of Electrical Engineering, The Hong Kong Polytechnic University, Hong Kong. His major research interests include the big data analysis, deep-learning algorithm, deep reinforcement learning algorithm, operation and planning of smart grid systems, hybrid energy storage system, and V2G service.

Paul Jen-Hwa Hu is David Eccles Chair Professor at the David Eccles School of Business, the University of Utah. He received his Ph.D. in Management Information Systems from the University of Arizona. His research interests include information technology for health care, business analytics, digital transformation, technology implementation and management, and technology-empowered learning and knowledge communities. Hu has published in various IEEE journals and transactions, Management Information Systems Quarterly, Information Systems Research, Journal of Management Information Systems, Decision Sciences, Journal of Medical Internet Research, Journal of Biomedical Informatics, Communications of the ACM, and ACM Transactions on Management Information Systems.

Chenghong Gu was born in Anhui province, China. He received the bachelor's and master's degrees in electrical engineering from Shanghai University of Electric Power and Shanghai Jiao Tong University, Shanghai, China, in 2004 and 2007, respectively, and the Ph.D. degree in electrical engineering from the University of Bath, Bath, U.K., in 2010. He worked with DECC U.K. to quantify the value of demand response to the energy system under 2050 pathways. He was involved in the design of the network pricing method—long-run incremental cost pricing (LRIC) for Western Power Distribution, which was adopted by the wide U.K. power industry. He was an EPSRC Research Fellow with the University of Bath. He is a Reader with the Department of Electronic and Electrical Engineering, University of Bath.

His major research interests include power economics and markets, multivector energy systems, and smart grid planning and operation. Dr. Gu is a Subject Editor for the IET Smart Grid.

Shuai Lu (S'17-M'21) received his B.S. degree in Smart Grid Information Engineering from Nanjing University of Science and Technology, Nanjing, China, in 2016 and his Ph.D. degree in Electrical Engineering from Southeast University, Nanjing, China, in 2021. From 2018 to 2019, he was a visiting scholar at the University of New South Wales, Sydney, Australia. He is currently a Lecturer at the School of Electrical Engineering, Southeast University.

He is the Young Editor Board member of Applied Energy. He was selected as an Outstanding Reviewer for IEEE Transactions on Power Systems in 2020. His research interests include multi-energy systems, operations research, and data-driven techniques in power systems.

Shixing Ding received his M.S. degree in Power Engineering from North China Electric Power University, Beijing, China, in 2019. He is currently pursuing a Ph.D. degree in Cyber Science and Engineering at Southeast University, Nanjing, China.

His research interests include modeling, simulation, and optimization of integrated energy systems; CPS security for energy systems.

Zhidong Cao received his Ph.D. degree at Institute of Geographic Sciences and Natural Resources Research, Chinese Academy of Sciences in 2008. He is currently a full professor and doctoral supervisor of the Institute of Automation, Chinese Academy of Sciences and the School of Computer and Control Engineering, University of Chinese Academy of Sciences, Beijing, China. He received the National Funds for Distinguished Young youths in 2020. Prof. Cao serves as a member of the expert group of the Joint Prevention and Control Mechanism of the COVID-19 Epidemic. He is a committee member, director, and standing director of numerous national societies.

His research direction includes big data-based social computing, public health emergency management, and spatial-temporal statistical analysis.

Da Xie was born in Heilongjiang province, China. He received the B.S. degree from Shanghai Jiao Tong University, Shanghai, China, in 1991; the M.S. degree from the Harbin Institute of Technology, Harbin, China, in 1996; and the Ph.D. degree from Shanghai Jiao Tong University, in 1999.

He is currently a Professor in the Department of Electronic Information and Electrical Engineering, Shanghai Jiao Tong University. His major research interests include multi-vector energy systems, electrical system simulation, power electronic equipment, and smart grids.

Yue Xiang received the B.S. and Ph.D. degrees from Sichuan University, China, in 2010 and 2016, respectively. From 2013 to 2014, he was a joint Ph.D. student at the Department of Electrical Engineering and Computer Science, University of Tennessee, Knoxville, US, a visiting scholar at the Department of Electronic and Electrical Engineering, University of Bath, UK in 2015, and also a visiting researcher at Department of Electrical and Electronic Engineering, Imperial College London, UK in 2019-2020.

Now he is an associate professor in the College of Electrical Engineering, Sichuan University, China. His main research interests are distribution network planning and optimal operation, power economics, electric vehicle integration and smart grids.